UNIVERSITAT POLITÈCNICA DE VALÈNCIA

ESCUELA TÉCNICA SUPERIOR INGENIERÍA INDUSTRIAL VALENCIA

INDUSTRIAL ENGINEERING MASTER THESIS

DESIGN AND IMPLEMENTATION OF A DEVICE FOR AUTOMATED MANAGING OF INLET AND OUTLET FLOWS IN A SYSTEM OF MULTIPLE MINI-BIOREACTORS

AUTHOR: NATHAN BEYER

SUPERVISOR: FERNANDO NÓBEL SANTOS NAVARRO

SUPERVISOR: PROF. JESÚS PICÓ MARCO

Academic year: 2020-21

Abstract

With the help of biotechnology, it is possible to produce metabolites of interest (e. g. amino acids, biofuel, drugs) in cells that are cultured in bioreactors. This project seeks to design and implement a millifluidic board system to automate the tasks of fresh medium feeding, volume control and sampling for a small scale (10 ml to 100 ml) laboratory bioreactor system for use in synthetic biology applications. After reviewing the state of the art, validation prototypes are designed and implemented to test the manufacturing process and the basic functions of the millifluidic boards. The manufacturing process consists of preparation of the material with adhesive, laser processing and the assembly. After calibration of the peristaltic pump, experimental tests of the validation prototypes are carried out to validate the system and to improve the design and manufacturing process. Subsequently, a prototype for controlling four bioreactors in parallel is designed and manufactured. A simulator is developed to compare different control strategies and parameters for experiments which use the millifluidic system. The simulator allows choosing any number of bioreactors to control thus making it applicable to a wide range of experimental setups. Finally, the scalability aspects of the system are discussed.

Keywords: Millifluidics, Biotechnology, Simulation, Laser processing, Automation, Peristaltic pump

Resumen

Con la ayuda de la biotecnología, es posible producir metabolitos de interés (por ejemplo, aminoácidos, biocombustibles, fármacos) en células cultivadas en biorreactores. Este proyecto busca diseñar e implementar un sistema de placas de milifluídica para automatizar las tareas de alimentación de medio fresco, control de volumen y muestreo para un sistema de biorreactores de laboratorio de pequeña escala (10 ml a 100 ml) para su uso en aplicaciones de biología sintética. Tras revisar el estado del arte, se diseñan e implementan prototipos de validación para probar el proceso de fabricación y las funciones básicas de las placas de milifluídica. El proceso de fabricación consiste en la preparación del material con un adhesivo, el procesamiento mediante una cortadora láser y el montaje de las placas. Tras la calibración de la bomba peristáltica, se realizan pruebas experimentales de los prototipos de validación para validar el sistema y mejorar el diseño y el proceso de fabricación. Posteriormente, se diseña y fabrica un prototipo para controlar cuatro biorreactores en paralelo. Se desarrolla un simulador para comparar diferentes estrategias y parámetros de control para los experimentos que utilizan el sistema milifluídico. El simulador permite elegir cualquier número de biorreactores a controlar, lo que lo hace aplicable a una amplia gama de configuraciones experimentales. Finalmente, se discuten los aspectos de escalabilidad del sistema.

Palabras clave: Milifluídica, Biotecnología, Simulación, Procesamiento por láser, Automatización, Bomba peristáltica

Contents

Abstract iii

Contents v

I Memoir 1

1 Introduction 3

2 Literature Review 5

2.1 Nano-, Micro- and Millifluidics . . . 5
2.2 Manufacturing processes for millifluidic channels . . . 6
2.2.1 Photolithography and soft lithography . . . 6
2.2.2 Additive manufacturing . . . 7
2.2.3 Laser processing . . . 9
2.2.4 Milling . . . 9
2.3 Valve technologies for millifluidic systems . . . 10
2.3.1 Miniature solenoid valves . . . 10
2.3.2 Integrated membrane valves . . . 11
2.4 Control of fluidic systems . . . 12
2.4.1 Hardware control . . . 12
2.4.2 Software control . . . 13
2.5 Modelling and control of microbial growth in bioreactors . . . 14
2.5.1 Bioreactor model . . . 14
2.5.2 Optical density control . . . 15
2.5.3 Growth rate control . . . 16

3 Validation prototype 17

3.1 Selection of valve type and manufacturing process . . . 17
3.2 Design . . . 18
3.3 Manufacturing and setup . . . 19
3.3.1 Laser processing . . . 19

3.3.2 Assembly . . . 22
3.3.3 Calibration of the peristaltic pump . . . 23
3.4 Test strategy . . . 27
3.4.1 Visual check of the valve functionality . . . 27
3.4.2 Basic board functionality test . . . 27
3.4.3 Flow selection test . . . 28
3.4.4 Dead volume handling . . . 28
3.4.5 Endurance test . . . 29
3.5 Validation prototype testing . . . 29
3.5.1 PETG prototype manufactured by Archicercle . . . 29
3.5.2 PMMA prototype 1 . . . 31
3.5.3 PMMA prototype 2 . . . 33

4 Simulator for biological experiments using a millifluidic system 37
4.1 Simulation model . . . 37
4.2 Fluid management strategies for biological experiments . . . 40
4.2.1 Interval strategy (IS) . . . 40
4.2.2 Highest demand strategy (HDS) . . . 40
4.2.3 Highest demand minimum quantity strategy (HDMQS) . . . 41
4.3 Identification of the optimal fluid management strategy for an experiment with four bioreactors . . . 41
4.3.1 Experiment parameters . . . 41
4.3.2 Evaluation method . . . 42
4.3.3 Results . . . 43

5 Prototype for four bioreactors 45
5.1 Design . . . 45
5.2 Functionalities . . . 46
5.3 Manufacturing and assembly . . . 47

6 Scalability 49

7 Conclusion and outlook 53

Bibliography 55

II Budget 59

8 Budget 61
8.1 Budget breakdown . . . 61
8.2 Workforce . . . 65
8.3 Total cost of the project . . . 65

III Drawings 67

9 Drawings 69

Part I

Memoir

Chapter 1

Introduction

With the help of biotechnology, it is possible to grow cells synthetically and to tailor their properties according to one's own needs by modifying the genes. For example, amino acids, propellants and medicine can be produced. In this context, one speaks of the "cell as a factory".

The players in the biotechnology industry are striving to maximize the production volume and the efficiency of the manufacturing processes which normally take place in bioreactors. Challenging aspects are the modeling as well as the measurement and estimation of important parameters of the process. Furthermore, the design of control laws that take into account the metabolic state of the cells is a significant challenge. Prior to setting up production on an industrial scale, the above steps are usually performed iteratively in small scale research bioreactors in order to develop satisfactory processes and determine parameters. Between small scale reactors used purely for research and development processes and the industrial reactors, an intermediate stage exists: mini-bioreactors with volumes of 10 to 100 ml which are the focus of this work. They are used for the characterization of synthetic biological circuits and serve the purpose of scaling up very small research reactors to industrial mass production. Often, many of these reactors are operated in parallel (e. g. 32 or 64) to investigate the influence of different parameters or to reduce the effect of statistical outliers on the results. Commercially offered solutions for these purposes are very expensive and usually not very flexible which makes their use impossible for many research groups or teachers. As an alternative, do-it-yourself (DIY) solutions are available, with examples provided by Wong et al. [Won+18] and Pilizota et al. [PY18]. The entry costs for suitable manufacturing processes such as 3D printing or laser cutting have fallen sharply in recent years, and the processes are available at many universities anyway. Electronic components such as sensors, small actuators, microcontrollers or microcomputers have also become more readily available while prices are falling. Open-source software libraries make it easier to program the systems. With DIY approaches, millifluidic reactor systems can be produced cheaply and quickly, enabling rapid adaptations and development cycles. A modular structure of the components ensures high flexibility.

One of the biggest costs of building a system of mini-bioreactors is the fluidic management of the substrates and bacteria, especially the fluidic components such as pumps and valves. In

a straightforward approach to fluid supply and removal, each reactor must be connected via tubing and a pump to each substrate that must be fed to it during the course of the experiment. In addition, depending on the design, there is one additional pump and hoses per reactor for removing excess volume or for taking samples from the reactors. The number of pumps and the effort required to lay lines thus scales linearly with the number of reactors. Without automation, the effort required to remove samples is also significant.

Therefore, this thesis will develop and prototype a fluidics control system for a set of bioreactors which requires significantly less tubing and pumps than the straightforward approach. The focus is on low-cost and flexible design which is why DIY processes and hardware are used. Initially, the system will be developed for experiments in four bioreactors with a volume of 15 to 20 ml, but later expansion to 8, 16, 32 or 64 bioreactors will be included. The system will allow control based on optical density and on the growth rate of the bacterial culture. In addition to feeding and automatic removal of excess volume, automatic sampling will be provided to minimize personnel time during the experiment run. Storage and allocation of samples into test tubes is not part of the work, samples are simply delivered to a certain outlet.

In the fundamentals part in chapter 1, differences between nano-, micro- and millifluidics are first worked out. This is followed by a description of various possible manufacturing processes for millifluidic devices. A further section deals with valves for controlling small volumes. The fundamentals part also includes the higher-level control of fluidic systems and the modeling of processes in bioreactors which are necessary for the development of a simulator. In chapter 3 a manufacturing process and a valve type are selected. Validation prototypes are designed and implemented to test the basic functions and to validate the design and the manufacturing process. Through the findings using the validation prototype, parameters for simulating biological experiments with the millifluid system are determined. The simulator is developed in chapter 4 and is suitable for any number of reactors. Using the simulator, different feeding strategies for an experiment with four bioreactors are tested and the best one is selected. Chapter 5 describes the design and fabrication of a prototype for feeding four bioreactors which can be used to run the simulated experiment from chapter 4 and validate the simulator. Chapter 6 discusses aspects of the scalability of the approach. Conclusion and outlook close the thesis.

Chapter 2

Literature Review

In this chapter, the state of the art regarding the fabrication and operation of millifluidic boards is elaborated. In section 2.1, millifluidics are distinguished from nano- and microfluidics. In section 2.2, several possible manufacturing processes for millifluidic devices are described. Two valve designs are explained in section 2.3. Section 2.4 deals with the control of fluidic systems in terms of hardware and software. Section 2.5 introduces a model of a bioreactor and two controllers for bioreactors.

2.1 Nano-, Micro- and Millifluidics

Nano-, micro-, and millifluidics refer to the science of manipulating, controlling, and studying fluids in channels or structures in the nano (1-100 nm) micro (1-100 µm) or millimeter (1 mm and larger) range [GL13; Kar18]. Figure 2.1 shows the indicated scales compared to naturally occurring things or things known from everyday life. The transitions between the ranges are fuzzy, other authors define microfluidics e. g. for sizes from 100 nm to 1 mm [Kit+12] or from 10 to 100 µm [ILH10]. In this context, the specified size refers to only one dimension, e. g. the width or depth of the channel or the diameter of the tube. Thus, microfluidic channels may well be several millimeters long [Kar18]. There is consensus on the definition of millifluidics as structures of 1 mm or larger in the crucial dimensions.

As the dimensions of the structures in which the fluids are studied decrease, the surface-to-volume ratio also decreases. Thus, the influence of surface tension becomes larger and the effect of gravity smaller. In addition, the Reynolds number decreases, making the flows laminar and eliminating turbulent effects. The behavior of the fluids is strongly changed compared to larger scales. It becomes clear, for example, when considering two parallel flows meeting in a microchannel: Due to the purely laminar flow, only slow mixing takes place at the contact surfaces caused by diffusion. For structures in the nanometer range, there are additional effects: The structures have the same order of magnitude as the molecules examined in them. Investigating these effects, with the goal of studying natural processes that take place in nanochannels, is one application of nanofluidics [Kar18]. Another application is the separation and determination of molecules,

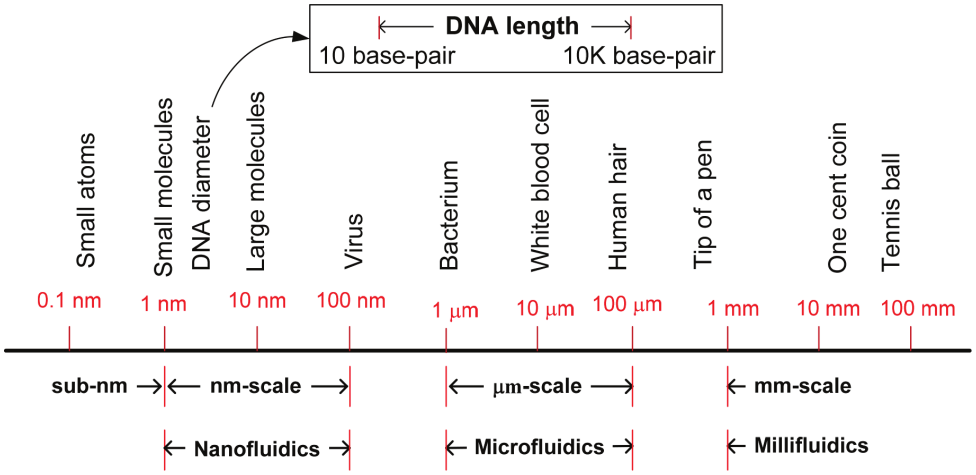

Figure 2.1: Scale of nano-, micro- and millifluidics compared to naturally occurring things or things known from everyday life. The boundaries and transitions are fuzzy. [Kar18]

e. g. to study proteins or DNA. In this way, small analytical devices that can be used quickly and flexibly can be manufactured, so-called "lab on a chip" [Esm+19].

Microfluidic systems take advantage of the specific flow properties on the one hand, and the ability to control small volumes on the other. The applications are diverse and in part similar to nanofluidics: they include, for example, analytical and synthetic chemistry, microbiology, biotechnology and diagnostic systems. Due to the small size of the systems, processes that would otherwise have to be carried out in a fixed laboratory can take place directly on site. The small volumes used can reduce reagent consumption and minimize costs. Microfluidics is also used where small volumes are unavoidable, such as for drug dosing or for dosing ink in inkjet printer printheads. [Kar18]

In contrast to nanofluidics and partly microfluidics, millifluidics can use manufacturing processes that are also common for devices with larger structures, such as 3D printing [Tsu+15], laser cutting [Won+18] or milling [Whi17](see also section 2.2). These processes are less costly than those used to fabricate e. g. nanofluidic devices, which is an advantage of millifluidics. The applications of millifluidics are diverse. Larger volumes, for example, allow analyses of whole cell cultures rather than individual cells to be performed in a lab on a chip. Millifluidics can also be used for droplet production and for analysis or control of small volume flows through valves [Tsu+15]. In the context of this work, only control by millifluidic systems will be applied.

2.2 Manufacturing processes for millifluidic channels

2.2.1 Photolithography and soft lithography

Photolithography is a process known from the manufacture of semiconductors and integrated circuits which can also be used for the production of nano-, micro- and millifluidic channels and structures. In this process, a wafer of silicon is coated with a photoresist. Rotational coating produces a uniform layer whose thickness depends on viscosity, rotational speed, acceleration and process time. The last three parameters can be selected to achieve the desired thickness.

The photoresist is then lightly cured in the oven. In the next step it is hardened in the desired areas using a photomask. After a further curing process, the photoresist is developed: in the case of positive photoresist, the areas exposed to UV light are removed; in the case of negative photoresist, the areas not exposed are removed. Thus, layer thicknesses of up to 300 µm and high resolutions are achievable [Won+18, supp. information]. The process of photolithography is complex and must even be carried out in a clean room if high quality is desired.

The fluidic chips can either be created directly by photolithography or a negative mold can be created by photolithography and the soft lithography process, described for example in [XW98] and [Kim+08], is used to produce the chips. This has the advantage that the complex photolithographically produced molds can be used several times. Polydimethylsiloxane (PDMS) is usually used, which is mixed with a hardener. Before and after application to the negative mold, the mixture must be degassed by a vacuum pump. Then the PDMS is cured in the oven. After cooling, the elastic chip can be cut out of the usually round mold and removed from the silicone wafer. After punching the access holes to the channels, the chip is completed by bonding the surface with the structures by plasma treatment with a glass plate. This creates waterproof channels. Soft lithography is widely used for microfluidics applications [HQ03; Kim+08; Whi+01]. Access to the technology is simplified because a clean room is not necessarily required.

The combination of photolithography and soft lithography for the application for millifluidic structures is even more complex. Since only a layer height of about 300 µm is possible, several layers of photoresist have to be applied on top of each other which requires a very precise, replicable alignment of the photomask in addition to the additional steps. Moreover, the bonding processes are not suitable for bonding larger areas which are necessary for millifluidic devices. Another disadvantage is that for systems with integrated membrane valves (see also subsection 2.3.2), bonding in the area of the valves must be prevented, but this cannot be done in an automated manner using a CAD drawing or similar in the context of soft lithography. [Won+18, supp. information]

2.2.2 Additive manufacturing

Additive manufacturing (AM) or 3D printing refers to manufacturing processes in which material is applied step by step to create three-dimensional objects. The geometry is obtained directly from a 3D CAD data set [GKT16]. Many different AM processes exist for a variety of materials, most commonly plastics, metals, and ceramics. In micro- or millifluidics for biological or chemical applications, plastics are used almost exclusively, so the two processes most commonly used for plastics are described here: Fused Layer Modeling (FLM), also known by the trademarked brand name Fused Deposition Modeling (FDM) and Stereolithography (SLA).

For FLM, filaments of thermoplastic material are melted and applied layer by layer by extrusion through a nozzle in such a way that the desired geometry is created. Curing takes place by cooling. The usual resolution for FLM is between 0.1 and 0.25 mm [GKT16]. The principle of the process is shown in Figure 2.2a. Kitson et al. use FLM with polypropylene (PP) as the plastic to fabricate three different chemical reactors in [Kit+12]. The channels have a circular cross-section of 0.8 mm diameter. The reactors were successfully tested using chemical synthesis experiments. PP is a suitable material because it has good chemical resistance and, at 0.02 $ per gram, is much cheaper than PDMS used in soft lithography. In [Tsu+15], Tsuda et al.

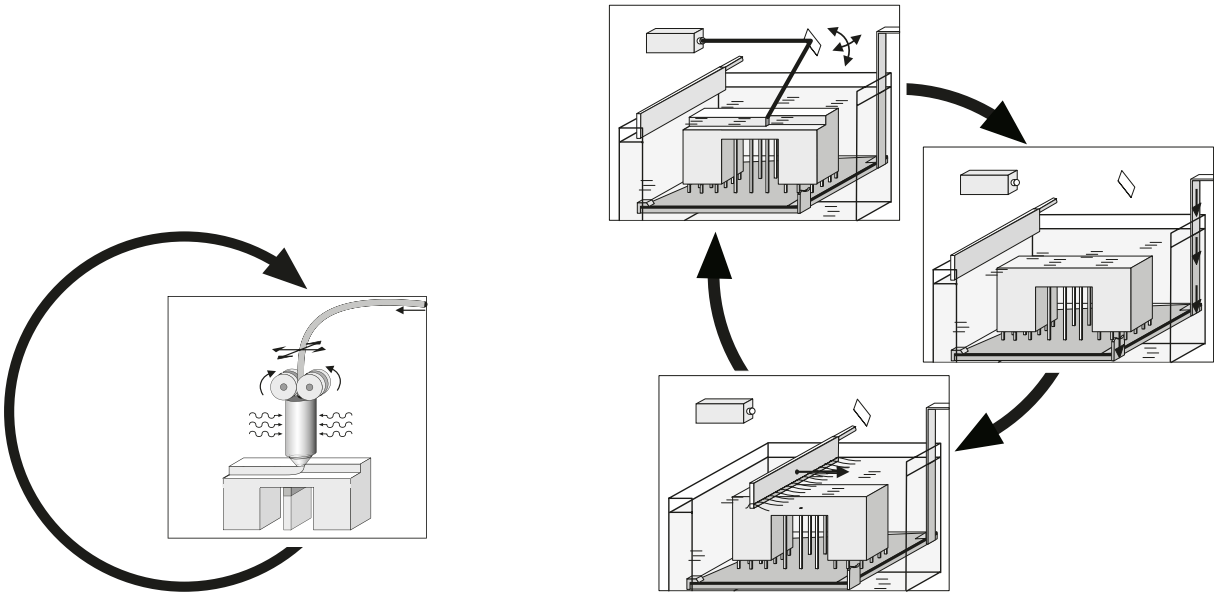

(a) Principle of the FLM process, in which plastic filament is melted and applied through a nozzle.

(b) Principle of the laser SLA process in three steps starting at the top left: Solidification of a layer, lowering of the platform and recoating of the component with resin.

Figure 2.2: Principle illustration of laser SLA and FLM. [GKT16]

use FLM with polyactides (PLA) as the material to fabricate various millifluidic devices for biological applications: two chips for droplet production, a chip with a reservoir for optical density measurement by an LED and a photoresistor, a device consisting of two 3D-printed components with an integrated membrane valve made of PDMS to select between two volume flows (see also subsection 2.3.2) and more. The channel dimensions, depending on the axis, range from 800 to 1200 µm. Male and female connectors were also printed to produce modular systems. Without further processing, the surfaces produced by FLM are too rough to ensure tightness between connectors. After vapor deposition with dichloromethane (DCM), the surfaces were smooth enough to demonstrate the possibility of tight connection of 3D printed parts by Tsuda et al. In [Mor+16], Morgan et al. investigate for FLM the deviations between CAD model specified and real channel dimensions at targeted heights and widths of 0.5 to 1.5 mm. They consistently achieve deviations of less than 2.5 %. Morgan et al. also fabricate modular fluidic systems. Unlike Tsuda et al., tightness is achieved via O-rings between male and female connectors here.

SLA is the oldest AM technology. Here, the platform on which the part is built is in a bath of the liquid monomer. The platform can be moved in the build direction (z-direction). According to the CAD data set, a light source which can be controlled in the x- and y-directions locally solidifies the liquid monomer by polymerization. The light source can be a UV laser beam controllable by a mirror or a UV projector selectively irradiated by a digitally controllable mask (e.g. LCD). After completion of a layer, the platform is lowered (irradiation from above) or raised (irradiation from below) by a layer thickness, according to the design of the printer. As is the case with FLM, support structures are necessary depending on the component design. After printing is complete, the component is washed to remove remaining monomers and fully cured in a UV chamber. The principle of laser-based SLA is shown in figure 2.2b. SLA produces parts with

smooth surfaces and high levels of detail [GKT16]. The utility of SLA for micro- and millifluidics has been demonstrated several times. Bhargava et al. [BTM14] developed a set of standardized, cube-shaped millifluidic components that can be modularly connected to form arbitrary systems. The components are fabricated using SLA and have channel dimensions ranging from 0.5 to 1 mm. Zhu et al. [Zhu+15] compare different additive manufacturuing technologies for fabricating fluidic devices for zebrafish embryo testing. A studied channel dimension of 500 µm could be reproduced by SLA with deviations between 0 and 2 %. The optical transparency, which is important for some applications, was better than other AM methods and comparable to soft lithography with PDMS. Shallan et al. [Sha+14] achieved channel dimensions as small as 250 µm using a conventional SLA printer for 2300 $ in the fabrication of a micro-mixer, gradient generator and droplet generator.

2.2.3 Laser processing

In laser cutting, the material to be cut is heated locally by a laser beam to such an extent that it is liquefied or sublimated, depending on the material. The liquefied material or the vapors from sublimation are removed by a process gas flowing out through the cutting nozzle at high speed. With sublimation, the cut edge becomes burr-free and smooth because no material residue remains; this case is also referred to as laser sublimation cutting. Typical materials for this process are plastics. If the traversing speed and power of the laser tool head are set appropriately, material removal with defined depths is also possible without completely cutting through the workpiece (laser engraving or structuring). This makes it possible to produce channels on the surface, and the process is suitable in principle for producing microfluidic or millifluidic systems. As with soft lithography and different from AM, the channel structure still has to be closed by gluing it onto a plate, since the channels can only be made on the surface. Wong et al. [Won+18] use laser engraving and cutting to fabricate a wide variety of millifluidic boards to control fluid supply and removal for systems with numerous bioreactors. In this case, structuring the surface without the possibility of fabricating internal channels is not a disadvantage: the boards each consist of two layers with a membrane in between to realize integrated membrane valves (see subsection 2.3.2). The material used is polyethylene terephthalate (PETG), a PET plastic modified with glycol.

2.2.4 Milling

Milling is a machining process with a geometrically defined cutting edge. Material is removed from the workpiece in the form of chips. The milling tool with one or more cutting edges rotates around its own axis. The cutting speed (rotational speed) and the feed rate are important parameters of the process. With automatic CNC milling machines commonly used today, complex geometries can be produced directly from a CAD model. Guckenberger et al. [Guc+15] present an overview and tutorial for the application of micromilling for the fabrication of plastic microfluidic components. They show the advantages and disadvantages compared to other popular and more well-known manufacturing processes such as SLA, injection molding, and hot stamping. The high processing speed of micromilling is particularly noteworthy: Components can be processed in minutes compared to often hours with SLA. Entry costs are high for high desired precision, but many universities already have a milling machine. In the fabrication of structures with around 1 mm size, Guckenberger et al. achieved deviations of less than 1 % using an entry-

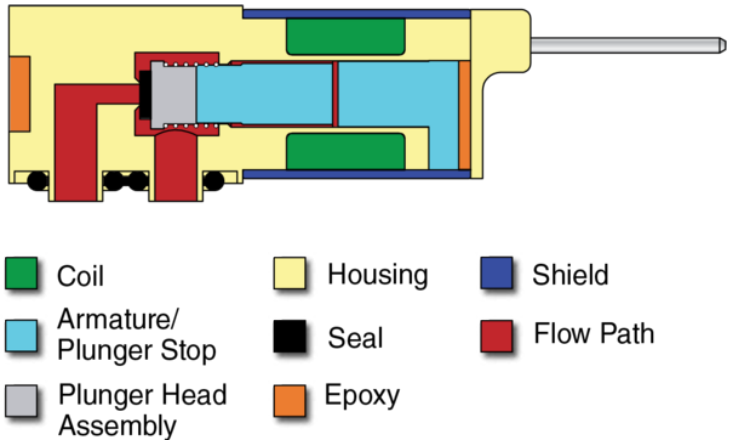

Figure 2.3: Schematic illustration of a miniature solenoid valve (part number LHDB0352115H) from The Lee Company. [The20]

level milling machine for 15000 $. In [Ali09], micromilling is also successfully used to produce structures from 500 to 800 µm in plastic. Lopes et al. [Lop+15] demonstrate the usability of micromilling to fabricate channels as small as 30 µm width to separate blood cells. As with AM and soft lithography, micromilling cannot fabricate internal channels because it can only remove material superficially. In addition to making channels directly in a workpiece, micromilling can also be used to make molds for soft lithography. In this way, the time-consuming process of photolithography can be avoided. This application is shown, for example, by Ardila et al. in [Ard+15].

2.3 Valve technologies for millifluidic systems

Millifluidic systems form an intermediate size between microfluidic systems and conventional fluidics. In conventional, industrial applications, electromagnetically actuated valves are usually used as active valves. A variety of approaches exist for microfluidics. The actuation of active microfluidic valves can be classified as mechanical, non-mechanical and external. An overview can be found, for example, in [OA06]. Some of the technologies used in these neighboring areas are transferable, others are not. We therefore restrict ourselves here to techniques for which a use in millifluidics has already been shown.

2.3.1 Miniature solenoid valves

Solenoid valves are valves that are actuated by an electromagnet. There are many different designs. They belong to the group of valves with mechanical actuation. On the one hand, solenoid valves are standard in industrial applications, on the other hand, their use in microfluidics has also been documented for a long time, e.g. in [TJA79], but for integrated design. Small size external solenoid valves are also used in millifluidics, e. g. in [Kin+14]. They are sold by several manufacturers. For example, a model from The Lee Co. (part number LHDB0352115H) has dimensions of about 8 x 22 mm. A schematic illustration of this valve is shown in Figure 2.3. The valve shown is normally closed. The seal at the front of the piston is pressed by a spring onto the passage in the flow channel. If the valve is to be opened, a magnetic field is generated

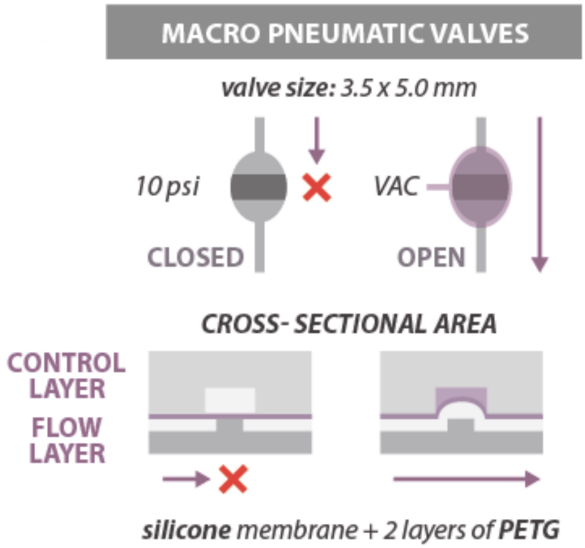

Figure 2.4: Schematic illustration of the operation of an integrated membrane valve. [Won+18, supp. information]

by the coil. The magnetic field exerts a force on the piston, which moves it backwards against the spring force and thus opens the flow channel.

2.3.2 Integrated membrane valves

Integrated membrane valves belong to the group of active, externally actuated valves. They are realized by a membrane between two functional layers. In the flow layer, the fluid to be controlled flows in channels; in the opposite control layer, air is used to actuate the valves. In the flow layer, there is a barrier at the valve. At high pressure in the control layer, the membrane is pressed against the barrier: the valve is closed. At low pressure (vacuum) in the control layer, the membrane lifts off the barrier and the valve is open. The operation is illustrated in figure 2.4 and has long been known for applications in microfluidics, e.g., in [VOE95] for channel widths as small as 200 µm. For millifluidic systems, the principle has been applied by Wong et al. [Won+18] to activate and deactivate a volume flow in individual channels. Volume flow rates of approx. $60\,\mathrm{ml\,min^{-1}}$ at channel widths and heights of 1 mm are applied. No significant leakage occurs at an air pressure of 0.7 bar for closed valves. Higher pressures are required for higher flow rates. To give the membrane in the valve area enough space to open, the channel geometry there is enlarged to an elliptical shape with the dimensions 3.5 x 5 mm. Silicone with a thickness of about 0.25 mm is used as the membrane material. Tsuda et al. [Tsu+15] use the same principle to implement valves for selecting a flow from multiple inputs. Since two layers, each with superficial channels, are connected for the integrated membrane valves, a manufacturing process that can only produce superficial structures such as soft lithography, laser cutting and micromilling is not a disadvantage.

The integrated membrane valves are made by bonding the control layer and the flow layer with the membrane in between. For some materials, no adhesive is necessary; activation of the surfaces of the control and flow layers by plasma treatment is sufficient for a strong bond [Tsu+15]. Wong et al. [Won+18] use a transparent adhesive layer (3M, 8146-3) with 75 µm thickness between

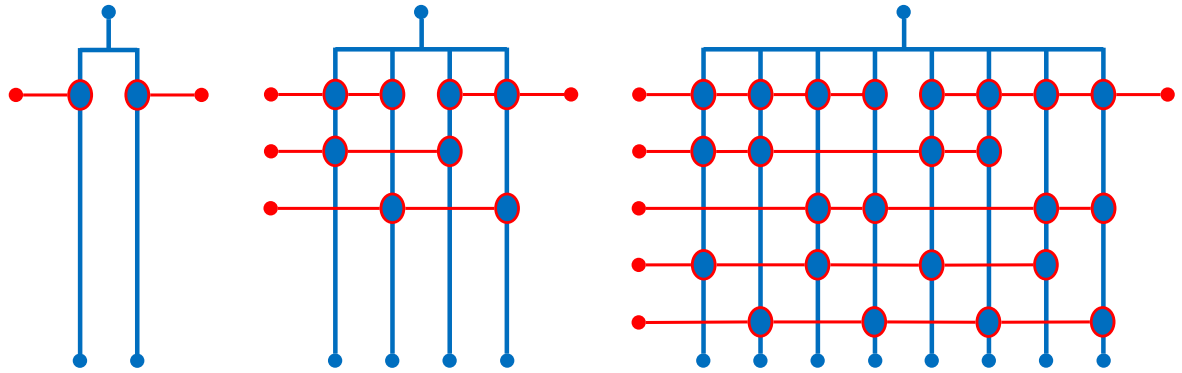

(a) Two lines **(b)** Four lines **(c)** Eight lines

Figure 2.5: Illustration of the necessary membrane valves (red-blue ellipses) and pneumatic connections (red circles) for the selection of exactly one line in a fluidic system with two, four and eight lines. The figure is adapted from the CAD design by Wong et al. [Won+18, supp. information].

the control layer and silicone membrane and between the flow layer and silicone membrane, respectively. To prevent the channels from being closed by the adhesive layer, it is applied before the laser cutting process. In both manufacturing processes, the silicone membrane must be prevented from sticking to the barriers in the valve area of the flow layer, otherwise the valve can no longer be opened. Tsuda et al. use a simple solution: during plasma treatment, the valve areas are masked with permanent marker to prevent bonding. The masking is removed during startup by flushing with ethanol. Wong et al. use the characteristics of the fabrication process for the channels: by setting the parameters for laser cutting to low power, the adhesive on the barriers is removed without affecting the plastic underneath. The markings for the barriers must be appropriately defined in the CAD model.

2.4 Control of fluidic systems

2.4.1 Hardware control

Control of the hardware is defined here as the control of the pumps and valves, since these are the active components that can influence the volume flows. The pumps can be controlled by appropriate electronic circuits. If miniature solenoid valves are used, they can also be opened or closed easily by applying a voltage. The integrated membrane valves are controlled by air pressure, whereby a vacuum must be applied to open them and a positive pressure to close them. A pneumatic valve that switches between the two pressure levels can therefore be used for control. When controlled by a microcontroller, electromagnetic pneumatic valves can be used here. The question arises here why solenoid valves are not used directly for the flow layer if the membrane valves in turn have to be controlled with solenoid valves. The advantage of membrane valves is that several can be controlled simultaneously with one air connection. By clever division of the membrane valves, fewer solenoid valves are needed for pneumatic control than lines for the fluids have to be controlled individually. This requires more membrane valves, but the manufacturing effort only increases with regard to the creation of additional cavities and the selective avoidance of bonding in the valve areas. This additional effort is purely machine-based when using the method of Wong et al. and is taken care of by the laser cutting machine.

Table 2.1: Number of necessary pneumatic solenoid valves for a certain number of lines to be controlled.

lines to control	necessary solenoid valves
$2^1 = 2$	$2 \cdot 1 = 2$
$2^2 = 4$	$2 \cdot 2 = 4$
$2^3 = 8$	$2 \cdot 3 = 6$
$2^4 = 16$	$2 \cdot 4 = 8$
$2^5 = 32$	$2 \cdot 5 = 10$
$\vdots$	$\vdots$
2^n	$2 \cdot n$

With the method of Tsuda et al., only more valve areas have to be masked with permanent marker.

Figure 2.5 shows how the number of necessary pneumatic connections and valves increases with the number of lines to be controlled. The part of the system shown is used to route an input to one of 2, 4 or 8 outputs. Two outputs require two pneumatic connections, four outputs require four, eight outputs require six, and 16 outputs require eight. For a doubling of the lines to be supplied, only two additional pneumatic connections and valves are required. Table 2.1 shows this behavior. Thus, with exponential increase of controllable lines, there is only linear increase of necessary solenoid valves.

2.4.2 Software control

Of the considered millifluidic devices and systems cited in this chapter, only Wong et al. [Won+18] discuss the control software architecture in more detail, so this approach is presented here.

In the work of Wong et al. the architecture of the control of the reactors and the fluidics is divided into three to four levels: on the lower level a SAMD 21 Arduino controls and monitors one parameter such as stirring, temperature and optical density or a function such as the control of the fluidics. For the latter, the Arduino can control up to 48 actuators for fluidics, i.e. pumps and valves, via an auxiliary board. This is done via three PWM boards with 16 channels each, which can amplify the output voltage of the Arduino and allow control by PWM on 16 channels, while the Arduino itself has only three PWM channels. In a simple fluidics setup, one pump is used per fluidics connection, so a total of up to 48 pumps are controlled and no valves. In the complex fluidics setup of Wong et al. one or more pumps and solenoid valves are controlled, which in turn actuate several membrane valves each (see also subsection 2.4.1). The fluidics Arduino translates abstract commands such as "Transport 3 ml of substrate A from the reservoir into reactor 8" into a sequence of commands for the pumps and valves involved. The abstract commands are received from the higher level via the RS485 serial communication protocol.

The layer above the Arduinos is a Raspberry Pi Linux board. The Raspberry Pi allows the system to communicate via standard Internet protocols. It monitors the Arduinos and notifies them of changes in desired parameters such as stirring speed and temperature or fluidics commands. It

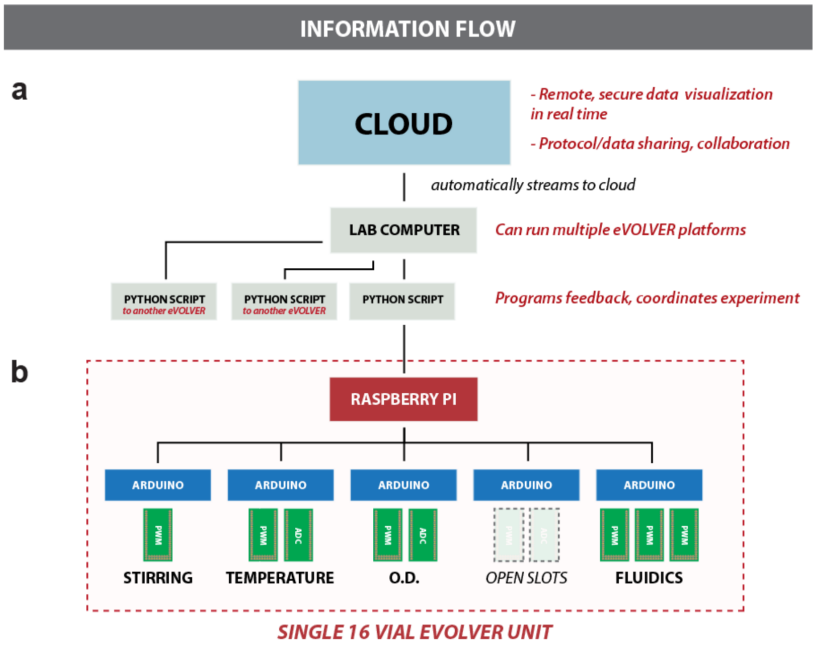

Figure 2.6: Software architecture of the millifluidic reactor system of Wong et al. which can be divided into four levels. [Won+18, supp. figure 3]

also receives sensor values from the Arduinos for display and analysis at a higher level. Together with the Arduinos, a Raspberry Pi forms a unit that can control up to 16 reactors.

The third layer of the system is formed by Python scripts that are executed on a laboratory computer. The scripts contain the parameters for the experiment to be performed. By copying the scripts, experiments can be easily replicated. The lab computer communicates with the Raspberry Pi via an Ethernet connection. One lab computer can control multiple units of 16 reactors simultaneously by running the Python scripts at the same time.

Optionally, the laboratory computers stream the data received from the reactor units to a cloud, which can be regarded as a fourth level. In this way, the experiments can be monitored and visualized remotely and a higher-level data evaluation of multiple experiments can be performed.

2.5 Modelling and control of microbial growth in bioreactors

2.5.1 Bioreactor model

For the simulation of the entire system with the millifludic system and the bioreactors, a model of the growth of microorganisms in bioreactors is necessary. In the experiments considered here, the solution in the bioreactors is constantly stirred and is thus homogeneous. In [BD91] the basic dynamics of such a system with one substrate to stimulate growth is described. The derivation is based on simple mass balances: For the biomass the equation is

$$\frac{\mathrm{d}(VX)}{\mathrm{d}t} = \mu V X - F_{\text{out}} X \tag{2.1a}$$

with the volume of the medium in the reactor V, the concentration of the microorganism (biomass) X in the reactor and in the effluent, the specific growth rate of the organism μ and the effluent flow rate F_{out}. For the substrate the following applies

$$\frac{\mathrm{d}(VS)}{\mathrm{d}t} = -k_1 \mu V X + F_{\text{in}} S_{\text{in}} - F_{\text{out}} S \tag{2.1b}$$

with the substrate concentration S in the reactor and in the effluent. The coefficient k_1 indicates how much biomass can be produced by how much substrate. The influent flow rate is denoted by F_{in}, S_{in} indicates the substrate concentration in the influent. The change in volume is given by the difference between influent and effluent flow rate

$$\frac{\mathrm{d}V}{\mathrm{d}t} = F_{\text{in}} - F_{\text{out}}. \tag{2.1c}$$

As an alternative to equation (2.1), the system can be described by introducing the dilution rate

$$D = \frac{F_{\text{in}}}{V} \tag{2.2}$$

with the equations

$$\frac{\mathrm{d}X}{\mathrm{d}t} = (\mu - D)X \tag{2.3a}$$

$$\frac{\mathrm{d}S}{\mathrm{d}t} = -k_1 \mu X + D\,(S_{\text{in}} - S) \tag{2.3b}$$

$$\frac{\mathrm{d}V}{\mathrm{d}t} = DV - F_{\text{out}} = F_{\text{in}} - F_{\text{out}}. \tag{2.3c}$$

One of the most important parameters for the system is the specific growth rate μ. It depends on a number of factors. One of the most commonly used models for the specific growth rate is the "Michealis-Menten law", also called "Monod law", which considers a dependence on the substrate concentration S:

$$\mu(S) = \frac{\mu_{\max} S}{K_{\text{M}} + S} \tag{2.4}$$

where $\mu_{\max}$ is the maximum growth rate and K_{M} is the Michaelis-Menten constant. [BD91]

2.5.2 Optical density control

An important output variable of the system is the optical density (OD) λ_{OD}. This, unlike the biomass or substrate mass, can be measured well using a light source and a photoresistor. It is calculated from the biomass using

$$\lambda_{\text{OD}} = \frac{X}{m_{\text{c}} n_{\text{OD}}}. \tag{2.5}$$

Here, m_{c} denotes the average cell mass in $^{\text{mg}}/_{\text{cell}}$ and n_{OD} is a conversion constant with unit $^{\text{cells}}/_{\text{ml}}$.

For the control based on the optical density with the influent flow rate F_{in} as manipulated variable, the control law

$$F_{\text{in}} = \frac{\lambda_{\text{OD}}\,\mu\,V}{\lambda_{\text{OD,ref}}} = \frac{\frac{X}{m_{\text{c}}\,n_{\text{OD}}}\frac{\mu_{\max} S}{K_{\text{M}}+S}}{\lambda_{\text{OD,ref}}}\,V \tag{2.6}$$

is applied.

2.5.3 Growth rate control

In addition to the optical density, it is often desired to control the growth rate μ. Here, a very simple controller is used to set the desired growth rate by a constant dilution rate. The control law is given by

$$F_{\text{in}} = \mu_{\text{ref}} V. \tag{2.7}$$

Chapter 3

Validation prototype

The goal of the validation prototype is to test the manufacturing process and the basic functions of the millifluidic system. The design and manufacturing process will be improved through an iterative approach. In section 3.1 the valve design and the manufacturing process are selected. In section 3.2, the design is explained. This is followed by the manufacturing process, assembly, and set up of the pump for testing in section 3.3. The test strategy for the validation prototypes is described in section 3.4. The test series for different variants of the validation prototype in section 3.5 concludes the chapter.

3.1 Selection of valve type and manufacturing process

Membrane valves are selected as the valve design principle of the millifluidic system. Using the method of Wong et al. described in subsection 2.4.1, fewer expensive solenoid valves are needed as fluid lines to be switched. Membrane valves allow manufacturing to be split into two layers. Both layers are each straightforward to manufacture. No solenoid valves need to be integrated into the millifluidic board.

The main advantage of photolithography and soft lithography is the high accuracy in producing structures in the micrometer range and the good reproducibility when producing several chips from one negative mold. A major disadvantage is the complex process for producing a master mold and the need for a clean room. This makes the process inflexible in terms of design changes. Since this project is aimed at building a millifluidic system rather than fabricating many identical chips, flexibility is more important than reproducibility, so the process is ruled out for fabrication. Furthermore, the method is best suited for layer thicknesses up to 300 µm, for millifluidic channels with e. g. 1 mm channel height, the application would thus be even more difficult (see also subsection 2.2.1).

AM offers a very high degree of design freedom. Interior structures can be created in a very simple way. The design flexibility is therefore very high. However, the choice of membrane valves means that only superficial channels with a depth of about one millimeter are required.

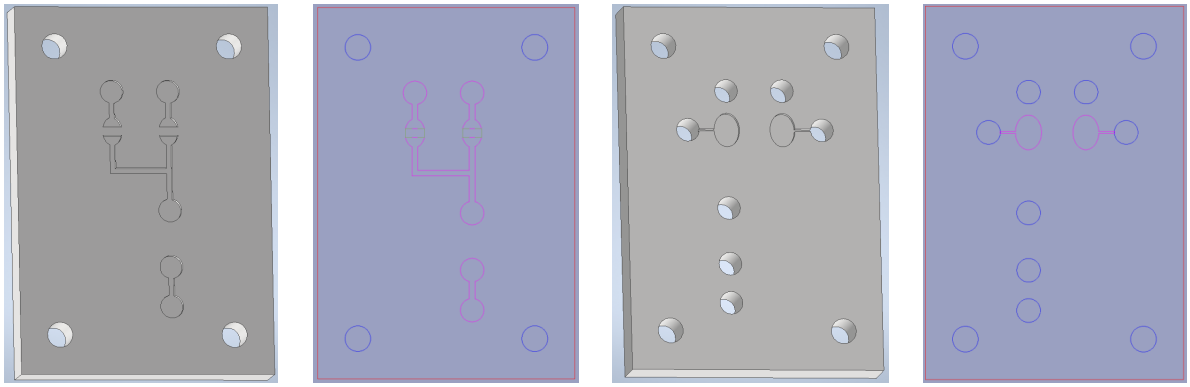

(a) Flow layer 3D design **(b)** Flow layer 2D design **(c)** Control layer 3D design **(d)** Control layer 2D design

Figure 3.1: CAD design in 3D (Autodesk Inventor) and 2D (Autodesk AutoCAD) of control and flow layer of the validation prototype.

Nevertheless, a thickness of the plastic plates for the control layer of 6 to 8 mm is necessary. In AM, the fabrication time increases sharply with the volume of material produced for the body. However, AM does not offer any advantages in generating the volume under the channels. Instead, the generation takes a very long time. In addition, depending on the AM process used, the surface quality is only average and the surface still needs to be reworked to produce membrane valves. For these reasons, AM is excluded as a manufacturing process for this project.

The two manufacturing processes remaining from those described in section 2.2, micromilling and laser machining, belong to the subtractive manufacturing processes. This means that material is removed from a basic geometry such as a rectangular plate to obtain the desired geometry. Since the millifluidic boards using membrane valves require little material to be removed for the channels and holes, these processes are ideal. With laser cutting, the workpiece does not have to be fixed in place because the process is contact-free. Since all production steps such as cutting, punching and engraving take place in one piece, no exact alignment of the workpiece is required. Because of these advantages over milling and the easier availability of the laser processing machine at the university, this process is selected.

3.2 Design

A simple Y-junction is produced for the validation prototype. Depending on the pump direction, two inputs and one output or one input and two outputs can be realized. In this way, the behavior when changing between two liquids can be investigated, or the distribution of a volume flow to one of two outputs. Since in later prototypes the choice from several liquids and the distribution to several outputs is implemented on one board and for this the pump is placed between the inputs and outputs, this is similarly dealt with for the first prototype. A parametric 3D model is created in the CAD software Autodesk Inventor Professional 2021. A 2D vector graphic is derived from the drawing of the 3D model. This is divided into different layers for holes, cuts, engravings for the channels and removal of the adhesive using Autodesk AutoCAD 2021 software. Each layer is then assigned appropriate parameters for the laser cutting process. The design is shown in figure 3.1.

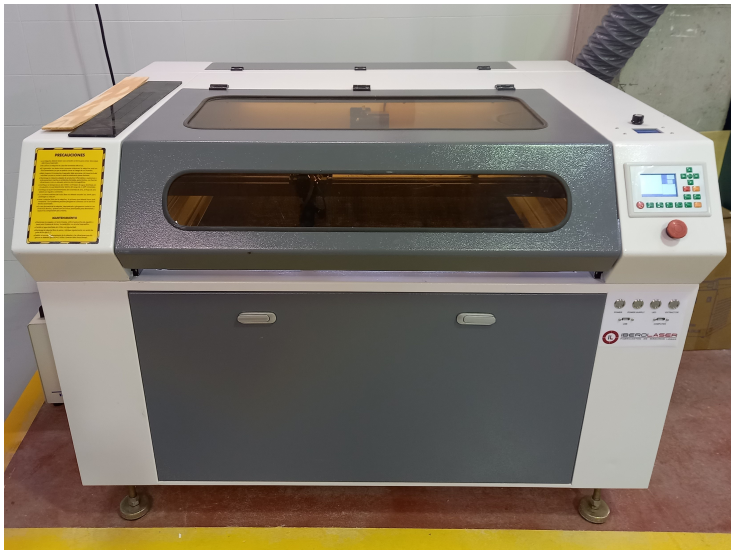

(a) Laser processing machine IL-9060.

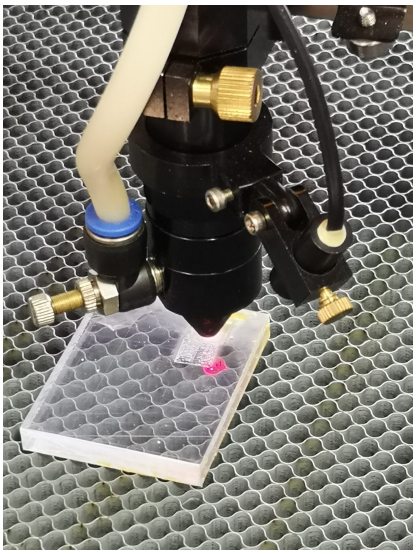

(b) Laser tool head.

(c) PETG cut edges.

(d) PMMA cut edges.

Figure 3.2: Laser processing machine, tool head and selected laser processing results.

3.3 Manufacturing and setup

3.3.1 Laser processing

The laser cutting machine is not available for the project from the beginning. Therefore, the first unit of the validation prototype is ordered for manufacturing from the company Archicercle in Valencia. There, only the laser machining process is carried out and not the assembly of the board.

The laser cutting machine of the Faculty of Fine Arts of the Polytechnic University of Valencia (UPV) can be used for the project later. It is the model IL-9060 of the manufacturer IBERO-LASER (see figure 3.2a). The machining area is 900 mm wide and 600 mm deep. The power of the CO_2 laser head (see figure 3.2b) is 90 W. Ambient air is used as cutting gas. The machine has an exhaust system. The machine is controlled by RDWorks software. Version V8.01.50-20200921 is used for the project. The manufacturing process is described in more detail below.

The adhesive is applied before the laser machining process. Thus, it is automatically trimmed at the edges and holes. In addition, the adhesive on the barriers in the valve areas can be removed automatically by the laser beam, which ensures the function of the valves. Application to the raw material takes place immediately after the protective film has been removed from the plastic to avoid dirt on the bonding area. If the protective film has already been removed, the surface must be cleaned before applying the adhesive. Adhesive tape is used to ensure an even layer thickness. After application, air bubbles under the adhesive must be removed by applying pressure with simultaneous movement from the center of the component outward. The pressure also improves the strength of the bonding. Initially, adhesive tape 3M 9088-200 with modified acrylic adhesive and polyester carrier is used as the adhesive. The adhesive tape has a thickness of 0.21 mm. According to the data sheet, it is used for materials with high and low surface energy. Due to the width of 50 mm, one strip is sufficient to cover the entire width of the validation prototype.

Later adhesive tape 3M 91022 is used with a special silicone adhesive and without a carrier. Due to the lack of a carrier, it is only 51 µm thick. Because of the high price, the tape is obtained in the width of 15 mm. This requires precise alignment with minimal spacing between strips to avoid leaks within the boards.

After application of the adhesive tape the laser processing is carried out. First, the correct distance of 8 mm between the processing head and the workpiece must be set using a gauge. The materials used are PETG in 8 mm thickness and polymethyl methacrylate (PMMA) in 6 mm thickness. Both are optically transparent. PETG has high resistance to a wide range of chemicals. In particular to highly concentrated ethanol which can be used to establish sterility in bioreactor systems. PMMA has lower resistance to highly concentrated ethanol. Stress cracks form in the case of permanent contact. On the other hand, PMMA is ideally suited for laser processing. The material sublimates when irradiated by the laser and thus leaves little or no trace on the workpiece. With PETG, it is more difficult to achieve sufficient quality during laser processing. The material melts during heating. Due to the high thickness, the cutting line is partially closed again by flowing and solidifying material. Thus, in some cases, a high force is required to release the components from the raw material or to remove the hole cutouts. In addition, the reject rate is significantly higher than with PMMA, since sometimes even post-processing cannot achieve sufficient quality. Furthermore, yellow residues are produced during processing, which are difficult to remove. Selected machining results for PETG and PMMA are shown in 3.2c and 3.2d. In addition to processing the flow and control layer, the holes and outer contours in the silicone membrane can also be fabricated with the laser.

The parameters for the various processing steps are determined by iterative adjustment and review of the results. The current for the laser and thus the power is adjusted on the one hand by the parameters in the software and on the other hand by a potentiometer on the machine. In table 3.1 the found parameters are shown. They are valid for the maximum current at the potentiometer. Minimum and maximum power can be set separately. For high cutting speeds and cuts with corners, the speed must be lowered near the corners so that the maximum acceleration is not exceeded. If the specification for the minimum power is different, the power is reduced according to the speed reduction. This ensures that all cutting areas are supplied with similar amounts of energy. Due to the low cutting speeds, it is sufficient to specify one power level here. In engraving, higher speeds are used, but the tool head is accelerated outside

Table 3.1: Laser processing parameters for different materials using the IL-9060 machine and RDWorks V8 software.

Output	Speed $mm\,s^{-1}$	Power (Min./Max.) %/%	Rep.	Mode	Scan mode	Interval mm
PETG, 8 mm thickness						
Outer cut	4.5	70/70	1	Cut	-	-
Holes	4.5	70/70	1	Cut	-	-
Engraving 1 mm	100	20/20	10	Scan	X-Swing	0.2
Engraving 1.3 mm	100	20/20	12	Scan	X-Swing	0.2
Engraving 1.6 mm	100	20/20	14	Scan	X-Swing	0.2
Adhesive removal	85	20/20	3	Scan	X-Swing	0.2
PMMA, 6 mm thickness						
Outer cut	6	70/70	1	Cut	-	-
Holes	6	70/70	1	Cut	-	-
Engraving 1 mm	90	20/20	8	Scan	X-Swing	0.2
Engraving 1.3 mm	90	20/20	10	Scan	X-Swing	0.2
Engraving 1.6 mm	90	20/20	13	Scan	X-Swing	0.2
Adhesive removal	85	20/20	2	Scan	X-Swing	0.2
Silicone membrane, 0.2 mm thickness						
Holes	40	20/20	1	Cut	-	-

the areas to be machined and the laser is then switched on at the right time. That is why only one power level is specified in this case. The mode determines whether a line is traced (Cut) or a surface is scanned (Scan). The Scan Mode determines the scanning axis (X or Y) and whether scanning is done in both directions (X-Swing) or only in one direction (X-unilateral). The Scan Interval determines how large the feed rate is between the scanning movements in the axis perpendicular to it. The high number of repetitions for engraving is selected so that only a small amount of energy is input per pass and the material does not melt.

3.3.2 Assembly

First, a clean and well-lit working environment must be provided. The following components and tools are necessary:

- Laser processed flow layer with adhesive tape applied before laser processing
- Laser processed control layer with adhesive tape applied before laser processing
- Silicone membrane of 0.2 mm thickness and surface area of minimum 65x45 mm
- 4 pcs. M4x25 screw
- 4 pcs. M4 nut
- 8 pcs. plain washer for M4 screws
- Trimming knife
- Tools to tighten the screws
- 2 pcs. steel plates
- Clamp
- Two component adhesive
- 7 pcs. barbed connectors

In the first step, the trimming knife is used to remove any impurities and residues in the channels from the flow and control layer. In the second step, the adhesive cover film is removed from the flow layer and the silicone membrane is applied. Wrinkles must be avoided during this process. Small bubbles can be pressed out with a bank card, for example. If the holes in the membrane for the passages to the flow layer were made with the laser processing machine, the 3D-printed assembly supports can be used to align the membrane correctly. If the membrane has not been prepared, holes for the passages must be cut with the trimming knife. Due to the elasticity of the silicone, round holes are difficult to implement manually, which is why the membrane is only cut in a cross shape. After gluing the membrane, it must be cut all around with the trimming knife to the geometry of the board. If not already done for the silicone membrane, the four assembly supports are passed through the holes at the corners of the flow layer. Alternatively, other round objects with 4 mm diameter like steel bolts can be used. Now, the cover foil is removed from the adhesive of the control layer and the control layer is positioned and pressed exactly on the flow layer with the membrane using the assembly supports. For better bonding, the assembly supports are removed and pressure is applied on both sides for 24 hours using a clamp via two steel plates. Then the control and flow layer are additionally connected with four screws, nuts and washers. In the final step, the adapters for the hose connections are attached. The fast-curing epoxy resin adhesive Loctite EA 3430 is used for this. During the process, no adhesive must get into the opening of the adapter.

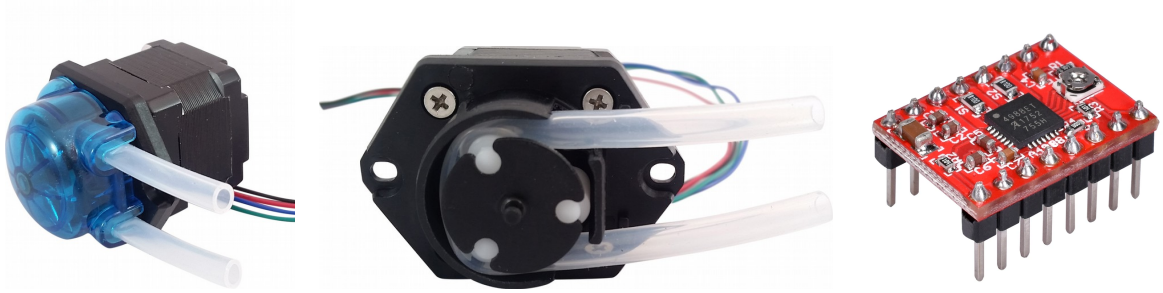

(a) Pump with cover (blue). **(b)** Pump without cover. **(c)** Stepper motor driver.

Figure 3.3: Peristaltic pump XP88-ST01 [Mas21] and stepper motor driver A4988 [BIQ21] used for the millifluidic system.

Table 3.2: Volume per revolution of the peristaltic pump XP88-ST01 for different tube inner diameters according to the data sheet [Mas21].

Tube inner diameter in mm	Volume per revolution in ml
2	0.145
3	0.275
4	0.440

3.3.3 Calibration of the peristaltic pump

A peristaltic pump is used for the millifluidic system. In this type of pump, the medium to be pumped is forced through a tube by external, mechanical deformation of the tube by means of rollers. Usually, the rotational movement for the deformation is generated by an electric motor. Here, a pump with stepper motor of type XP88-ST01 is used. The stepper motor achieves higher precision than other electric motors. In the model used, the peristaltic motion is generated by three rollers spaced 120° apart. For one rotation 200 steps are necessary. Thus, one step corresponds to 1.8°. For continuous load, the pump is allowed up to speeds of $200\,\mathrm{min}^{-1}$. To move the motor one step a rising edge at the corresponding input of the motor driver is necessary. The minimum period per step results from the maximum speed of $200\,\mathrm{min}^{-1}$ by:

$$200\,{}^{\text{rounds}}/_{\text{min}} \mathrel{\widehat{=}} 40000\,{}^{\text{steps}}/_{\text{min}} \mathrel{\widehat{=}} 666,6\overline{6}\,{}^{\text{steps}}/_{\text{s}} \mathrel{\widehat{=}} 1500\,{}^{\mu\text{s}}/_{\text{step}} \tag{3.1}$$

This minimum period can be divided, for example, in each 750 µs high and low level. Tubing with an inner diameter (ID) of 2 to 4 mm and a wall thickness of one millimeter can be used for the pump. Table 3.2 shows the displacement per revolution for the different ID according to the data sheet. For $200\,\mathrm{min}^{-1}$ and 4 mm ID, this results in a maximum flow rate of $88\,\mathrm{ml\,min}^{-1}$. The pump is shown in figures 3.3a and 3.3b.

An Arduino MEGA2560 and a driver of type A4988 are used to control the stepper motor. The driver supports voltages from 8 to 35 V and can provide a resolution up to one sixteenth of a step. If desired, the field effect transistors (FETs) or all electronics can be disabled by the Arduino. In this way, heat generation can be avoided and the motor and electronics can be protected in phases without operation. However, the position of the motor is not held this way and can change when force is applied. The driver is shown in figure 3.3c.

Table 3.3: Parameter overview for the peristaltic pump calibration measurements.

Mark	without mark	*	**	+
Time per step in ms	5	5	1.5	5
Nr. of steps per set of steps	5, 10, 20, 50, 100, 200	200	200	[66,67,67]
ID of the tube in mm	2	2	2	2
Tube outlet	pipette tip	pipette tip	pipette tip	pipette tip
FETs disabled in idle state	no	yes	yes	no

For calibration, distilled water is pumped from a storage container into another container, the weight of which is measured with a precision balance. The density is approximately $1\,\mathrm{kg\,l^{-1}}$, which is why weight and volume can be considered equal. The experimental setup for the calibration is shown in Figure 3.4a. Volumes are examined for performing 5, 10, 20, 50, 100 and 200 steps at a time. After each set of steps, the new weight in the target container is recorded. Of each set of steps, 60 repetitions are performed, so as to cover the complete working range of the pump and to reduce the influence of random deviations. In addition, the average deviation of the volumes from the mean value can be determined in this way. The next set of steps is triggered by closing a contact on the breadboard, resulting in a high level at the corresponding digital input of the Arduino. Silicone tubing with 2 mm ID is used for the pump since high accuracy is prioritized over high flow rate. To avoid influence of oscillations and vibrations, the measurements are initially performed with a period per step of 5000 µs, which corresponds to a speed of $60\,\mathrm{min^{-1}}$. The FETs remain permanently active. Measurements are also made with deactivation of the FETs between sets of steps at 5000 µs period (denoted by *) and at maximum speed with a period of 1500 µs (denoted by **). Another configuration consists of one set of steps with 66 steps followed by two sets of steps with 67 steps (marked +). This attempts to use symmetry in the mechanical structure with three rollers with 120° spacing. An adapter is first attached to the outlet of the tube to the measuring container (see figure 3.4b) to reduce the inner diameter and reduce droplet formation. Nevertheless, especially for small sets of steps, the influence of droplet formation is large. Therefore, a pipette tip with a different geometry and significantly smaller outlet diameter is used instead of the adapter (see figure 3.4c). With this configuration, no droplets formed at the outlet during calibration. Table 3.3 shows the parameters for the different calibration measurements. An extract of the raw data of the measurements with the pipette tip can be found in table 3.4.

On the raw data, significant deviations from the mean value in the transported weight per set of steps can be seen in the measurement series for less than 200 steps per set of steps. The average deviation is given in table 3.5 in row c) and amounts to several milligrams in each case. In percentage terms, the deviation is between 9 % for 100 steps per set of steps and 56 % for 5 steps per set of steps (see table 3.5 row d)). Looking at the raw data, it is noticeable that the deviations are composed of two components. The first component is random deviations of at most one to two milligrams from the mean. These can be caused, for example, by small air bubbles in the tubing, formation of very small droplets at the pipette tip or measurement inaccuracies of the balance. The second and larger component is the dependence of the pumping behavior on the current angle of the stepper motor. The behavior can be observed well at 50 or

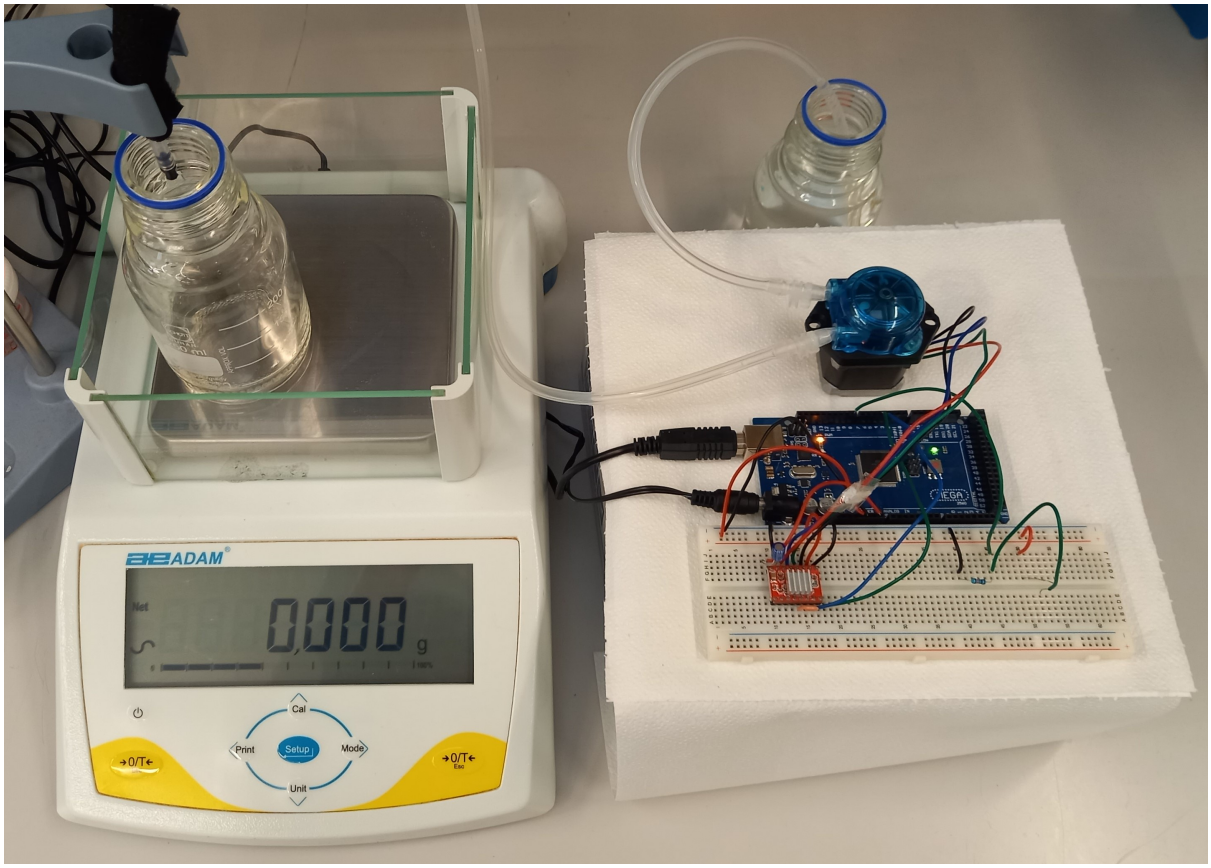

(a) Overview of the experimental setup.

(b) Tube with adapter.

(c) Tube with pipette tip.

Figure 3.4: Experimental setup for calibration of the peristaltic pump.

Table 3.4: Raw data of the calibration of the peristaltic pump: weight gain in the target container per set of steps performed.

Weight gain in milligrams in the target container per set of steps performed.									
Set of steps number	Number of steps per set m								
	5	10	20	50	100	200	200*	200**	$66.\bar{6}^{+}$
1	6	0	3	30	97	180	179	180	57
2	7	2	24	55	74	180	184	180	59
3	6	12	24	47	105	180	182	178	61
4	6	15	10	37	82	180	181	182	59
5	4	12	17	39	98	180	182	180	57
6	2	11	27	54	81	181	181	180	61
7	-1	7	13	50	99	179	183	180	58
8	0	0	7	36	82	182	181	181	60
9	-1	3	25	40	98	180	182	180	59
10	7	14	24	54	82	181	182	180	59
11	4	13	3	49	95	181	180	180	58
12	9	12	23	36	83	178	182	181	59
13	4	11	28	40	98	181	182	180	58
14	6	2	7	55	81	181	183	180	60
15	6	3	18	46	99	180	179	182	60
16	7	12	27	38	82	180	182	180	58
17	4	9	14	40	99	181	183	179	58
18	6	14	8	53	81	180	180	180	61
19	0	11	26	48	96	180	182	181	60
20	1	11	24	38	82	180	182	180	59
21	1	2	2	40	100	181	182	180	59
22	0	0	22	55	82	180	181	181	59
23	2	13	27	47	99	180	181	179	57
24	6	13	9	37	81	181	182	180	62
25	5	13	18	39	98	180	182	182	57
26	7	11	26	54	82	181	181	178	59
27	7	8	14	48	98	181	183	180	58
28	6	0	7	37	81	179	182	180	60
29	7	3	26	41	98	182	180	180	58
30	6	13	23	55	82	180	182	179	60

Table 3.5: Statistical parameters of the calibration of the peristaltic pump: a) Mean weight per set of steps in milligram. b) Mean weight per step in milligram. c) Mean deviation to mean weight per set of steps in milligramm. d) Mean deviation to mean weight per set of steps in relation to mean weight per set of steps, without unit.

Statistical parameter		Number of steps per set m								
		5	10	20	50	100	200	200*	200**	$66.\bar{6}^{+}$
a)	$\frac{\sum_{i=1}^{n} x_{i,m}}{n} = \bar{x}_m$	4.15	8.68	17.58	44.56	89.71	180.36	181.65	180.2	58.65
b)	$\frac{\sum_{i=1}^{n} x_{i,m}}{n\,m} = \bar{\bar{x}}_m$	0.830	0.863	0.879	0.891	0.897	0.902	0.908	0.901	0.880
c)	$\frac{\sum_{i=1}^{n} \lvert x_{i,m} - \bar{x}_m \rvert}{n}$	2.335	4.557	7.625	6.600	8.407	0.794	0.831	0.667	1.030
d)	$\frac{\sum_{i=1}^{n} \lvert x_{i,m} - \bar{x}_m \rvert}{n\,\bar{x}_m}$	0.5627	0.5248	0.4337	0.1481	0.0937	0.0044	0.0046	0.0037	0.0176

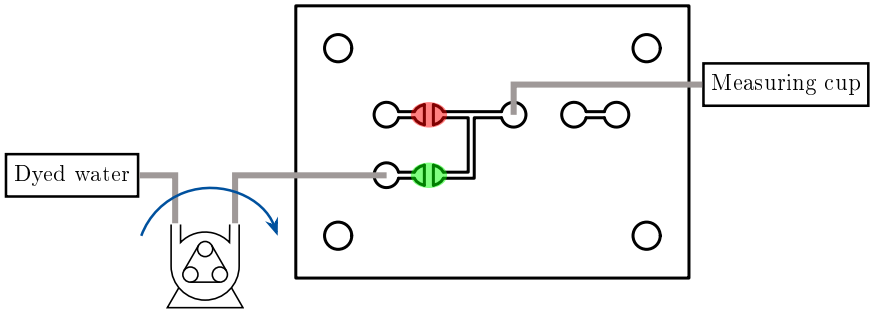

Figure 3.5: basic board functionality test schematics

100 steps per set of steps. Here, for every fourth respectively second set of steps, the transported weight varies only within the limits of the random deviations. For the other, smaller step set sizes, the pattern repeats itself accordingly, only with a different frequency. In the measurements for 200 steps per set of steps, which corresponds to one revolution, the angle-related deviations are omitted and the deviation from the mean value is only 0.67 to 0.83 mg and 0.37 to 0.46 %, respectively. Measurements for 200 steps per set of steps with the FETs turned off between steps do not yield a significantly worse result. At higher speed (measurement with **) the accuracy even reaches its best value of 0.37 %. At the same time, this significantly reduces heat generation by the pump and driver and prevents overheating. The average pumped weight per revolution is 180.2 mg when measured at high speed. Measurement with one-third of a revolution per set of steps (one time 66 and two times 67 steps) also provides quite high accuracy with 1.76 % while maintaining a high resolution of the transported weight of 58.65 mg per set of steps on average.

3.4 Test strategy

The tests are aimed at ensuring that the quality of the manufacturing process is sufficient. In addition, the function of the valves and the behavior of the fluids in the channels are to be examined. With the validation prototype, errors can be identified and resolved more easily than with more complex prototypes.

3.4.1 Visual check of the valve functionality

In this test, the basic function of the valves is checked visually. For this purpose, a vacuum and pressure are alternately applied to the air connection of the valve. It is observed whether a lifting of the silicone membrane can be detected when vacuum is applied and whether the membrane sinks when pressure is applied. Detection from the outside may be difficult due to the furrows caused by the laser machining process.

3.4.2 Basic board functionality test

This test checks the basic function of the validation prototype for a simple fluidic operation. It is tested whether a volume flow can be realized from one of the two inputs via a valve and the output to a measuring container. So the following points are checked:

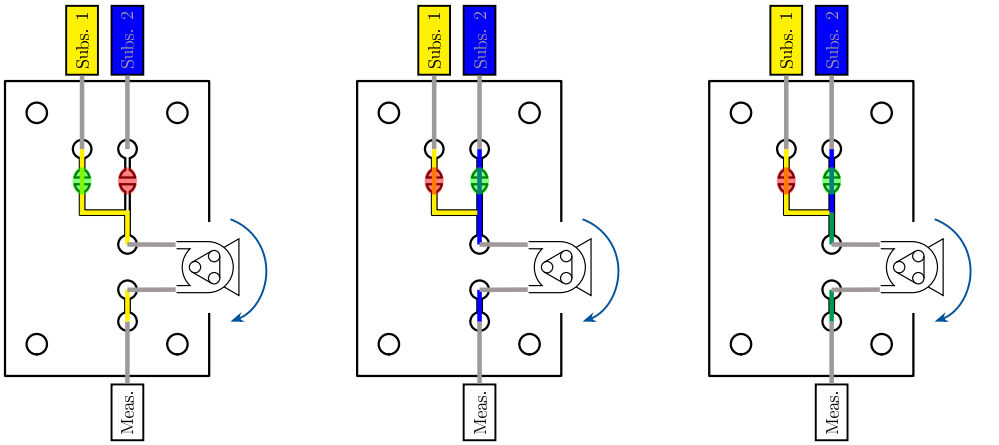

(a) Begin of the experiment.

(b) Desired behavior after input change.

(c) Possible behavior directly after input change.

Figure 3.6: Flow selection test.

- Opening of the valve through which the volume flow is realized.
- Closing of the valve through which the volume flow shall not flow.
- Tightness of the board during volume flow.

The test procedure is shown schematically in figure 3.5 on page 27.

3.4.3 Flow selection test

During the operation of millifluidic boards for biological experiments, it may be necessary to switch between several substrates as input for different reactors. The validation prototype will be used to investigate how the fluids in the channels behave during this process. It is about the crossing of the two inputs. It will be analyzed whether fluid from the input of the old substrate still enters the volume flow of the new substrate when switching between two substrates. This could make it necessary to first empty the channel of the old substrate before inserting the new substrate. This would mean that an air inlet would be necessary for each substrate inlet. For the test, colored water is used again. Figure 3.6a shows the first step of the experiment. The desired behavior after switching is shown in Figure 3.6b. Behavior like in Figure 3.6c should be avoided if possible.

3.4.4 Dead volume handling

For substrate distribution to the reactors, high accuracy in dosing is required. However, the volume of the lines must be taken into account during supply. These must first be filled before volume is dispensed to the reactor. Thus, more must be pumped than ultimately arrives at the reactor. One solution to this problem is to pump exactly the desired volume from the corresponding inlet, then switch to the medium air and displace the volume through the air in the ducts and hoses until the ducts are emptied again and the complete desired volume has arrived in the reactor. The purpose of this test is to see if it is possible to displace the volume all the way into the reactor by air without the liquid getting stuck at any point in the board. A prerequisite for accurate metering of the substrates is that the lines from the inlets to the

intersection with the inlet for air are fully filled. The test in the previous subsection shows whether this is possible.

3.4.5 Endurance test

In biological experiments, the millifluidic board is used for many hours. In addition, the boards should also be able to be used for several experiments. It must be ensured that the board is leak-proof. In particular, it is important that the flow layer, the control layer and the silicone membrane do not delaminate, i.e. that the bonding does not fail. For this purpose, a volume flow of $36\,\mathrm{ml\,min^{-1}}$ (maximum speed) is pumped through one of the two channels with valve for five minutes. The procedure is repeated for the channel with the other valve. Colored water is used so that it is easier to see when liquid enters between the layers of the board. The setup regarding the pump is the same as for the basic board functionality test from subsection 3.4.2 shown in figure 3.5.

3.5 Validation prototype testing

3.5.1 PETG prototype manufactured by Archicercle

The prototype made of PETG by Archiercle shows the typical problems of laser processing of this material. In the figures 3.7a and 3.7b, the partially unclean cut edges and engravings can be seen. For the assembly of this prototype, the silicone membrane is not prepared by the laser processing machine and therefore not yet perforated. After applying the membrane to the flow layer, access to the channels is created by cutting a cross into the membrane in the appropriate area. A screw clamp in conjunction with steel plates is not yet used here for bonding. Instead, pressure is built up on the bonding by strongly tightening the screw connections in the corners. The fully assembled prototype is shown in figure 3.7c. The experiments are performed in a pneumatic laboratory of UPV, where air pressure, vacuum as well as pneumatic control are available. For volume transport the peristaltic pump is used which was set into operation and calibrated in subsection 3.3.3.

First, the visual valve test from subsection 3.4.1 is performed. When switching between vacuum and pressure, no movement of the silicone membrane is visible in the valve area. However, the view is limited by the uneven engraving in the valve area. Thus, there may be movement that is not visible from the outside. The result of the valve test is thus unclear. Possible causes for a malfunction may be:

- The silicone membrane crossed with the trimming knife is sucked to the 3D-printed adapter by the vacuum and closes it, so that there is no vacuum in the valve chamber.
- The channels in the control layer for the air from the inlets to the valve chamber are too small and not deep enough.
- The vacuum is too weak.
- The silicone membrane sticks to the flow layer and therefore does not lift.

Next, the basic board functionality test from subsection 3.4.2 is performed. The experimental setup is shown in Figure 3.7d. Once the colored water enters the channels, a water film is visible

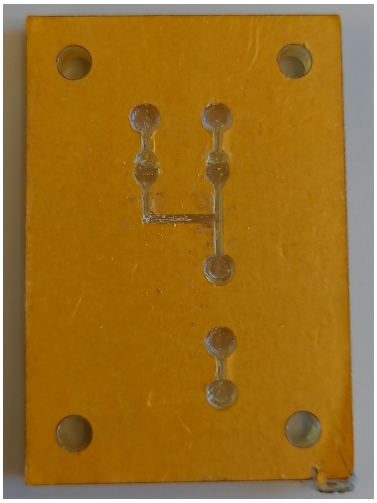

(a) Flow layer.

(b) Control layer.

(c) Assembled validation prototype.

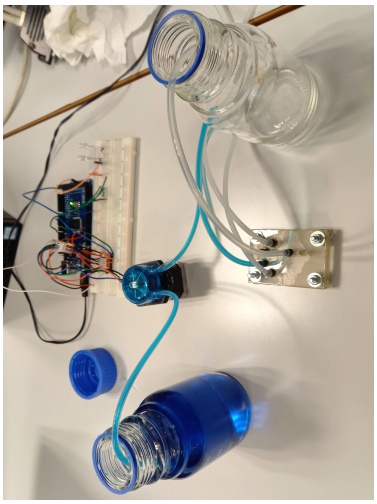

(d) Test setup with pump, arduino control, millifluidic board and dyed water as test liquid.

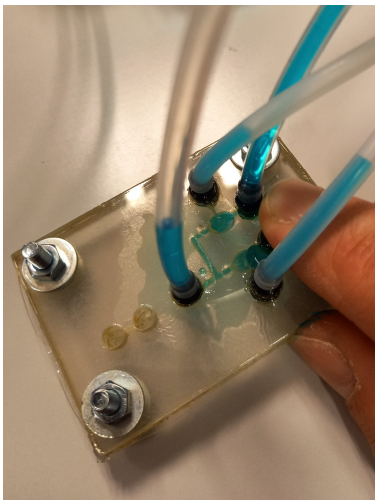

(e) Leakage to the air channels.

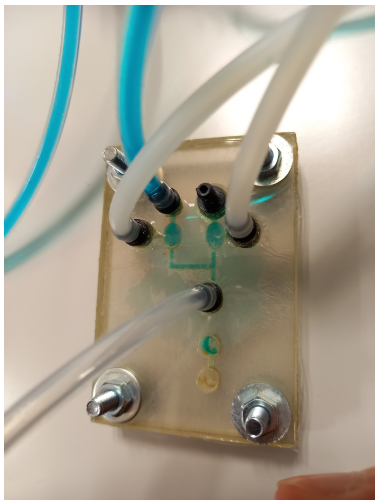

(f) Leakage.

Figure 3.7: Single layers, assembly and test of the validation prototype manufactured by Archicercle using PETG material.

between the control and flow layer. The water flows in the direction of the output, but still also in the direction of the closed valve. The colored water is also visible in the air hoses. At the hose under pressure, air leaks at the adapter connecting the 6 mm diameter air hoses of the pneumatic laboratory with those of the 4 mm diameter millifluidic system. Possible causes for the results of the test may be:

- The bond between the silicone and the adhesive is not strong enough and the bond loosens due to the pressure of the water.
- The vacuum in one channel of the control layer locally loosens the membrane from the adhesive under the channel, allowing water to enter between the two layers.
- Water gets into the air tubes through openings in the silicone membrane that were accidentally made at the control layer air ports during assembly.
- Excessive force due to the screw connections at the corner points lead to bulging.

Due to the total failure of the prototype in the basic board functionality test, no further testing will be performed. The actions derived from the tests with this prototype are described in the next subsection.

3.5.2 PMMA prototype 1

Due to the possible causes of the problems in the tests of the prototype made of PETG produced by Archicercle, the following changes will be made for the next prototype:

- PMMA instead of PETG as a material for better quality of laser processing.
- Increase of the width of the channels of the control layer from 0.5 to 1 mm.
- Change of the engraving depth of the control layer from 1 to about 1.6 mm to give the membrane more room to move to open.
- Change of the engraving depth of the flow layer from 1 to about 1.3 mm to facilitate volume flow and reduce pressure.
- Cutting the holes and outer contours of the silicone membrane with the laser processing machine.
- Bonding of the layers with the silicone membrane for a prolonged period of at least 24 hours under uniform pressure of plates, not screws.
- Light tightening of screw joints in corners.
- No accidental punching of the membrane at the holes for the control layer.

The improved quality of the laser processing of the flow and control layers compared to the previous prototype can be seen in figures 3.8a and 3.8b. On the assembled prototype in figures 3.8c and 3.8d, it can be seen that yellow discoloration as with PETG are avoided and sharp contours of the channels are achieved.

First, the visual valve test from subsection 3.4.1 is performed. When changing between pressure and vacuum, the rise and lowering of the silicone membrane in the valve area is clearly visible. The visual valve test is therefore successful.

The basic board functionality test from subsection 3.4.2 is then performed. A pressure of 0.7 bar is applied to the valve to be closed. A vacuum of about -0.25 bar is applied to the valve to

(a) Flow layer.

(b) Control layer.

(c) Assembled validation prototype.

(d) Rear side of the assembled validation prototype.

(e) Liquid routing with one valve under vacuum and the other valve under pressure.

(f) Liquid routing with one valve under vacuum.

Figure 3.8: Single layers, assembly and test of the first self-made validation prototype using PMMA material.

be opened. As seen in Figure 3.8e, the blue colored water flows to the desired outlet and not through the blocked valve. Unlike Archicercle's prototype, no fluid flows between the two layers. The fluidic channels of the flow layer are tight. The tightness is maintained even at the maximum flow rate of the pump for the entire test period of a few minutes. The leakage seen in the photos is between the hose and the connector and can possibly be prevented by using a cable tie. In principle, it does not affect the test of the board. The air pressure at the closed valve triggers a leakage between the control layer and the silicone membrane. In the area of the channels of the underlying flow layer, the membrane is lifted off the adhesive and moves into the channels of the flow layer. This causes air to escape from the connectors to the flow layer. This is due to inadequate bonding of the silicone. Due to the air flow in the tubes for the liquid, the volume flow cannot be well defined, which is why further improvements must be made to the validation prototype and the test series is stopped.

3.5.3 PMMA prototype 2

Due to leakage between the control layer and silicone membrane on the first prototype made of PMMA, the 3M 9088 double-sided adhesive tape is replaced by 3M 91022. The 3M 91022 adhesive tape is specially developed for silicone materials and promises higher adhesive strength on this material. The manufacturing and assembly process remains unchanged. Front and rear sides of the finished validation prototype are shown in figures 3.9a and 3.9b.

First, the visual valve test from subsection 3.4.1 is performed. When switching between pressure and vacuum, the rise and fall of the silicone membrane in the valve area is clearly visible for both valves. The visual valve test is therefore successful.

The basic board functionality test from subsection 3.4.2 is then performed. A pressure of 0.7 bar is applied to the valve to be closed. A vacuum of about -0.25 bar is applied to the valve to be opened. The colored water flows as desired from the inlet with the pump to the outlet of the validation prototype. No air bubbles appear in the hose at the outlet. There is no leakage of air in the control layer to the flow layer. This means that the silicone membrane does not separate from the adhesive, unlike the prototype from subsection 3.5.2. There is some fluid leakage. However, this leak is between the tubing and the adapters that connect the tubing to the board, not inside the board. Other adapters can prevent the leakage, but are not yet available when the project is carried out.

In the next step, the flow selection test from subsection 3.4.3 is performed. For this purpose, orange and blue colored water are used as test fluids. The setup is shown in figure 3.9c. First, the left valve is opened and the right valve is closed and the orange water is pumped to the outlet. This can be seen in figure 3.9d. Then the left valve is closed and the right valve is opened. The result can be seen in figure 3.9e. The orange water is forced back into the other channel at the junction about 5 mm. The leaking liquid is due to leaks between the hoses and the adapters, not leaks within the board. Large air bubbles are visible in the tubing at the outlet to the pump. These are also due to leaks between the hose and the adapter. Here, the liquid from the board is sucked in by the pump and not forced through, which is why the bubbles are caused by air entering. A leak of compressed air in the control layer can be excluded, since no further bubbles occur when the pump is stopped.

(a) Front side of the assembled board.

(b) Rear side of the assembled board.

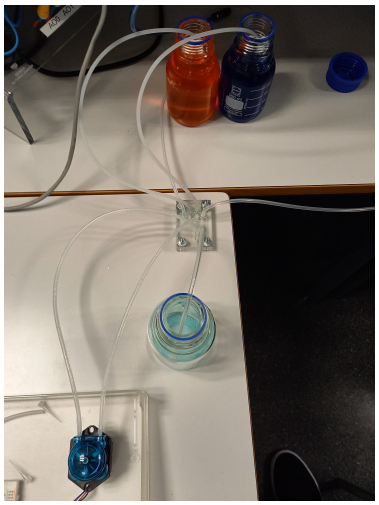

(c) Setup for the flow selection experiment.

(d) First phase of the flow selection experiment.

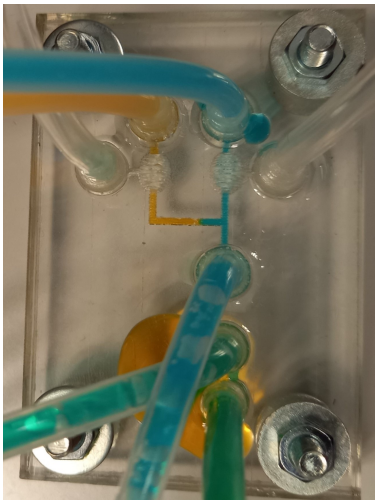

(e) Second phase of the flow selection experiment.

(f) Dead volume handling experiment.

Figure 3.9: Front and rear side, test setup and test results of the second self-made validation prototype using PMMA material and 3M 91022 adhesive.

The flow selection test is followed by the dead volume handling test from subsection 3.4.4. The test starts by pumping orange water through the board. Air is then pumped through the system in the same way. Figure 3.9f shows that a few residues of the colored water remain in the channels, but the channels are largely emptied. Eliminating the leaks between the hoses and adapters can probably improve the results. An alternative option is to apply compressed air to the channels, as this provides a higher volume flow of air compared to the pump and empties the channel even better.

As a final test, the endurance test from subsection 3.4.5 is performed for both valves. No leakage is detected in the board, so the test is successful.

Now that all tests of the validation prototypes have been carried out successfully, the manufacturing process and the basic functions of the millifluidic system approach are validated. These are the prerequisites for designing and building more complex prototypes as described in chapter 5.

Chapter 4

Simulator for biological experiments using a millifluidic system

In this chapter, a model for simulating biological experiments using a millifluidic system for fluid management is presented. The simulation model can be used to compare different fluid management strategies and parameters for different experiments. The simulator can be employed for the preparation of real biological experiments. Thus, the optimal fluid management strategy can be found without having to perform a real experiment many times. Due to the high preparation effort and long runtime of the real experiments, the simulator can save many resources. In section 4.1, the simulation model is explained. In section 4.2 the different fluid management strategies are presented. An example application of the simulator to determine the best fluid management strategy for an experiment with the millifluidic board from chapter 5 is given in section 4.3. The simulator models, scripts and functions can be found in the GitHub repository under `https://github.com/sb2cl/MilifluidicBoard`.

4.1 Simulation model

The simulation model for the millifluidic board and bioreactors is built in Matlab Simulink® and is shown in Figure 4.1. It is suitable for simulating various fluid management strategies in systems of any number of reactors. The OD or the growth rate can be chosen as the reference variable. Currently, only the supply of one substrate is considered.

At the top left of the model in the "References" area, the trajectories for the desired reference variable are fed into the model. The trajectories can be selected individually for each reactor. Any input signals can be applied. The figure shows a step function. The reference variable is selected via the variable `ref_select`.

The millifluidic system is modeled in the "Millifluidic board" area. The different fluid management strategies with one or two pumps are modeled by state transition diagrams. The strategies are described in section 4.2. As input variables, the controller receives the current

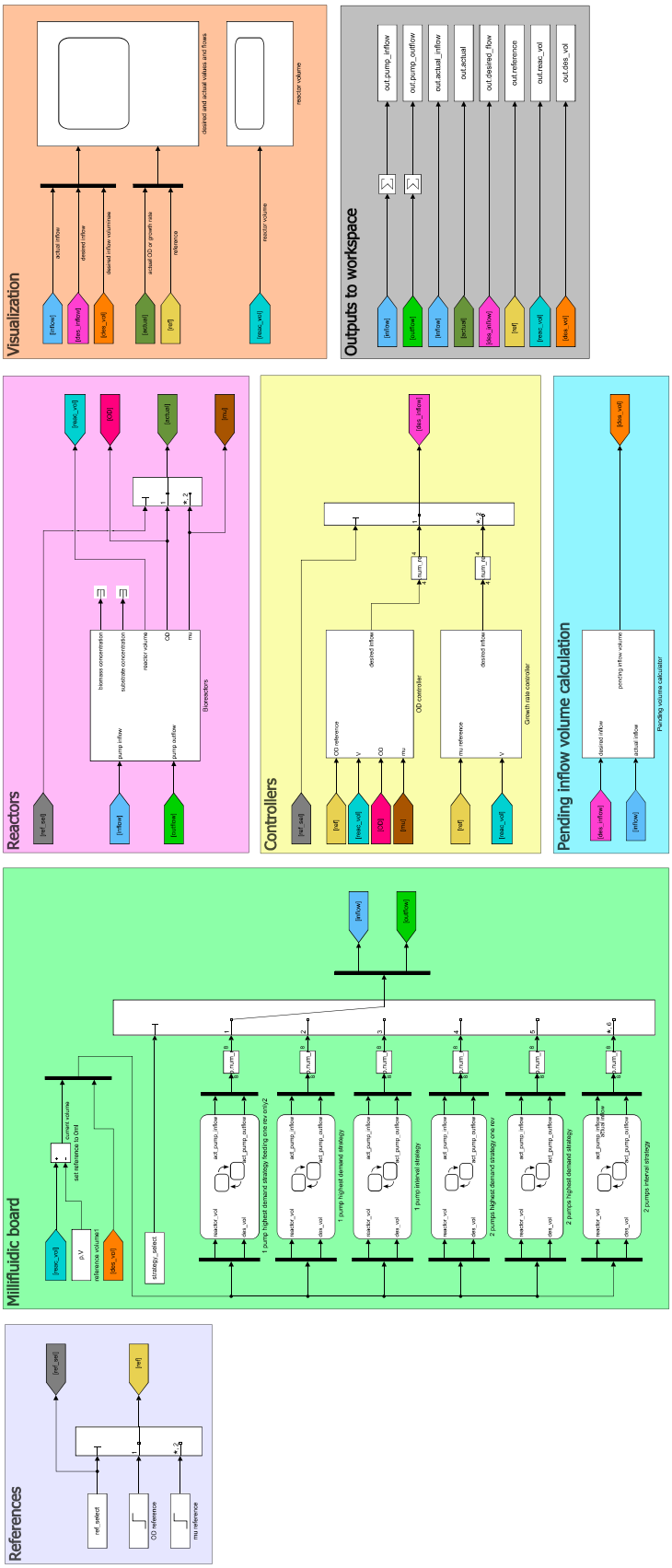

Figure 4.1: Simulink model for simulation of the millifluidic system for multiple bioreactors. Different feeding strategies and reference variables (OD and growth rate) can be selected.

volume in all reactors and the desired pending substrate volume for all reactors. The variable `strategy_select` is used to select the desired fluid management strategy for the simulation. Output variables are the inlet flow and the outlet flow of each reactor. Due to the switching structure of the membrane valves (open or closed), only one reactor can be supplied with fluid at a time. With two pumps, liquid can at the same time be pumped out of one reactor. There are no intermediate states, so that, for example, with two valves open, half the volume flow could flow through each line. The millifluidic system model takes into account sampling at the desired interval (`p.sampling_int`), the maximum volumetric flow of the pump (`p.max_pump_flow`), and the resolution of the pump (`p.pump_res`).

In the area "Reactors" the bioreactors are modeled. The differential equations are implemented vectorially, so that the dimension and thus the number of bioreactors (`p.num_reac`) can be changed as desired. Only the substrate inlet volume flow and the outlet flow are required as inputs. Outputs are biomass concentration, substrate concentration, volume in reactor, OD and growth rate. Depending on the selected reference variable, the OD or the growth rate is passed on for the evaluation.

The controllers for the OD from subsection 2.5.2 and for the growth rate from subsection 2.5.3 are implemented in the "Controllers" area. The controller for OD requires as inputs the OD reference, the volume in the reactors, the optical density, and the growth rate. The controller for the growth rate only needs the reference and the current volume in the reactor. The controller output used is switched depending on the reference variable selected. The controllers assume an ideal liquid supply and disposal. This means that at any time exactly the inlet flow desired by the controller can be made available. The outlet flow is always exactly large enough to maintain the reference volume of the reactors. Thus, in this ideal case $F_{\text{in}} = F_{\text{out}}$ applies. As described above, in the millilfluidic system, only one reactor can be supplied or have waste removed at a time. Thus, the controller output cannot be physically implemented directly.

For the substrate supply, the following procedure is used with this background: the inlet flow output by the controller is integrated in the "pending inflow volume calculation" area as long as the reactor is not currently being supplied. As soon as the reactor can be supplied, the pending desired volume is reduced. The intervals in which the desired volume is removed should be as short as possible in order to deviate minimally from the continuous implementation of the control law. Liquid removal is needed to keep the volume in the bioreactors constant and to automatically remove samples for analysis at specific time intervals. The current volume is one of the three state variables in the simulation model and is therefore known. The volume to be removed results from the difference between the actual volume and the reference volume of the reactor.

4.2 Fluid management strategies for biological experiments

Various approaches can be taken for the time allocation of the pump or pumps to the reactors, which are presented below.

4.2.1 Interval strategy (IS)

In the interval strategy, the reactors are allocated time windows of equal length in which the pump or pumps supply and remove waste from the reactor.

If two pumps are used, supply and waste removal take place at the same time. While the time window is active, substrate is pumped into the reactor active for supply until the pending desired volume is zero. At the same time, liquid is pumped out of the reactor active for waste removal until its reference volume is no longer exceeded. Once these tasks have been completed, the pumps stand still for the remainder of the time interval. In each case, an external counter for supply and waste removal specifies the change to the next reactor. The time interval for sample collection is a multiple of the interval for supply and waste removal. As soon as the time to the next desired sample removal has elapsed, the pump for waste removal changes to the mode for sample collection. In this mode, one sample is taken from each reactor in turn and made available at the outlet. For this strategy, the time interval (`p.interval`) is an important parameter.

If one pump is used, it must take care of both supply and waste removal. After intervals for the supply of all reactors, there are intervals for the waste removal of all reactors. Due to the architecture with one pump, biomass is partially pumped through pipes during waste removal, in which substrate is to be fed to the reactors again later. To prevent contamination of one reactor with cells from another reactor, these areas must be cleaned before substrate is fed again. Thus, a waste removal cycle is always followed by the cleaning program. During this time, the reactors cannot be supplied. Thus the system cannot be controlled. The cleaning time (`p.clean_time`) is therefore an important parameter that must be minimized. Before and after sampling, a cleaning procedure must also be performed.

4.2.2 Highest demand strategy (HDS)

With the highest demand strategy, the reactor with the largest pending volume is always supplied with substrate.

If two pumps are used, one pump is responsible for the substrate supply and the other for the liquid removal. For both supply and waste removal, the reactor with the highest demand is always controlled. For waste removal, this is the reactor whose actual volume is farthest above the reference volume. As with the interval strategy, sample removal via the pump for waste removal occurs at a desired time interval.

If only one pump is used, supply and waste removal must be performed by the same pump. In this case, the supply continues to be carried out on the basis of the highest demand. Waste removal strategy is changed. If waste removal was based on highest demand, there would be frequent changes between supply and waste removal of individual reactors. Each time there is a switch back to supply, the cleaning procedure would have to be performed. Therefore,

Table 4.1: Values of the reference trajectories with the OD as reference variable.

Reference	OD		
	Step time	Initial value	Final value
Reactor 1	500	0.1	0.5
Reactor 2	250	0.2	0.4
Reactor 3	600	0.5	0.1
Reactor 4	400	0.4	0.2

only volume is removed from the reactors as soon as a threshold (`p.waste_threshold`) above the reference volume is exceeded by one reactor. Then a cycle of waste removal is performed immediately so that the volume is lowered to the reference volume for all reactors. After that, interrupted by a cleaning procedure, the supply is resumed. Sample collection is performed at the defined interval. Since the threshold for waste removal strongly influences how often cleaning is necessary, it is an important parameter for this strategy.

4.2.3 Highest demand minimum quantity strategy (HDMQS)

In the highest demand minimum quantity strategy, the reactor with the largest pending volume is supplied with substrate. In contrast to the highest demand strategy, only the minimum quantity of substrate, i. e. the resolution of the pump, is supplied to the corresponding reactor. Then it is checked again which reactor has the highest demand.

When two pumps are used, this principle is followed for supply and waste removal. Samples are removed by the pump for waste removal at the desired time interval.

When using one pump, waste removal is triggered by exceeding a threshold for excess volume, as in the highest demand strategy. Regardless of demand, each reactor is then reset to the reference volume. After that, interrupted by a cleaning procedure, the supply is resumed. Sample collection is performed at the defined interval. Since the threshold for waste removal strongly influences how often cleaning is necessary, it is an important parameter for this strategy.

4.3 Identification of the optimal fluid management strategy for an experiment with four bioreactors

For the identification of the best fluid management strategy for an experiment with four bioreactors, we consider the prototype of the millifluidic system described in chapter 5. In this example, the optimal fluid management strategy for an experiment with OD as the reference variable is determined.

4.3.1 Experiment parameters

Different step functions with steps at different times are chosen as trajectories in each case. The values are given in table 4.1. The initial values for the states are chosen for all reactors as

Table 4.2: Parameters of the millifluidic system and their relevance to the different strategies.

Parameter	Value	Relevance to strategies					
		HDMQS 1P	HDS 1P	IS 1P	HDMQS 2P	HDS 2P	IS 2P
`p.num_reac`	4	x	x	x	x	x	x
`p.interval`	0.5 min			x			x
`p.max_pump_flow`	36 ml min^{-1}	x	x	x	x	x	x
`p.pump_res`	0.18 ml	x	x	x	x	x	x
`p.clean_time`	0.6 min	x	x	x	x	x	x
`p.waste_treshold`	3 ml	x	x				
`p.sampling_int`	15 min	x	x	x	x	x	x

follows:

$$X_0 = 0.1\,\mathrm{mg\,ml^{-1}} \qquad S_0 = 16\,\mathrm{mg\,ml^{-1}} \qquad V_0 = 15\,\mathrm{ml} \tag{4.1}$$

The parameters for the bioreactors are:

$$\mu_{\max} = 0.0289\,\mathrm{min^{-1}} \qquad k_1 = 1.43 \qquad K_\mathrm{M} = 0.1802\,\mathrm{g\,l^{-1}} \tag{4.2}$$

$$S_\mathrm{in} = 3.6\,\mathrm{g\,l^{-1}} \qquad n_\mathrm{OD} = 1 \cdot 10^9\,{}^{\mathrm{cells}}/_{\mathrm{l}} \qquad m_\mathrm{c} = 433 \cdot 10^{-12}\,{}^{\mathrm{mg}}/_{\mathrm{cell}} \tag{4.3}$$

The parameters for the millifluidic system are shown in table 4.2. Partially the parameters are not relevant for all strategies, this is also indicated in the table. As interval for the supply half a minute is chosen to supply the reactors on the one hand with short time interval and on the other hand not to have to switch the valves constantly as with an interval of e.g. three seconds. The volume of one complete revolution of 0.18 ml is used as resolution for the pump, since the highest accuracy was achieved in this case (see subsection 3.3.3). 0.6 min is chosen as the cleaning time for the system, which corresponds to 36 seconds. The exact cleaning time depends strongly on the performed cleaning procedure, the development of which is not part of this work. 3 ml is chosen as the limit value for switching to waste removal during operation with one pump. With a reference volume of the reactor of 15 ml and a capacity of 20 ml, there is still a tolerance of 2 ml before the reactor is fully filled. Sampling is scheduled every 15 minutes. For the simulation a fixed step size of $1 \cdot 10^{-4}$ min and the fixed step solver Runge-Kutta method of third order were used.

4.3.2 Evaluation method

For the evaluation of the fluid management strategies, the deviations of the OD from the ideal trajectory with the values $\lambda_{\mathrm{OD}_{k,\mathrm{id}}}$ are considered. The ideal trajectory means the trajectory if the controller output would be directly implemented by the fluidic actuator. The ideal trajectories and the reference trajectories for the OD are shown in Figure 4.2. For quantification, the mean error (ME)

$$\mathrm{ME} = \frac{1}{N} \sum_{k=1}^{N} \left| \lambda_{\mathrm{OD}_{k,\mathrm{id}}} - \lambda_{\mathrm{OD}_k} \right|, \tag{4.4}$$

is calculated, where N corresponds to the number of measured values.

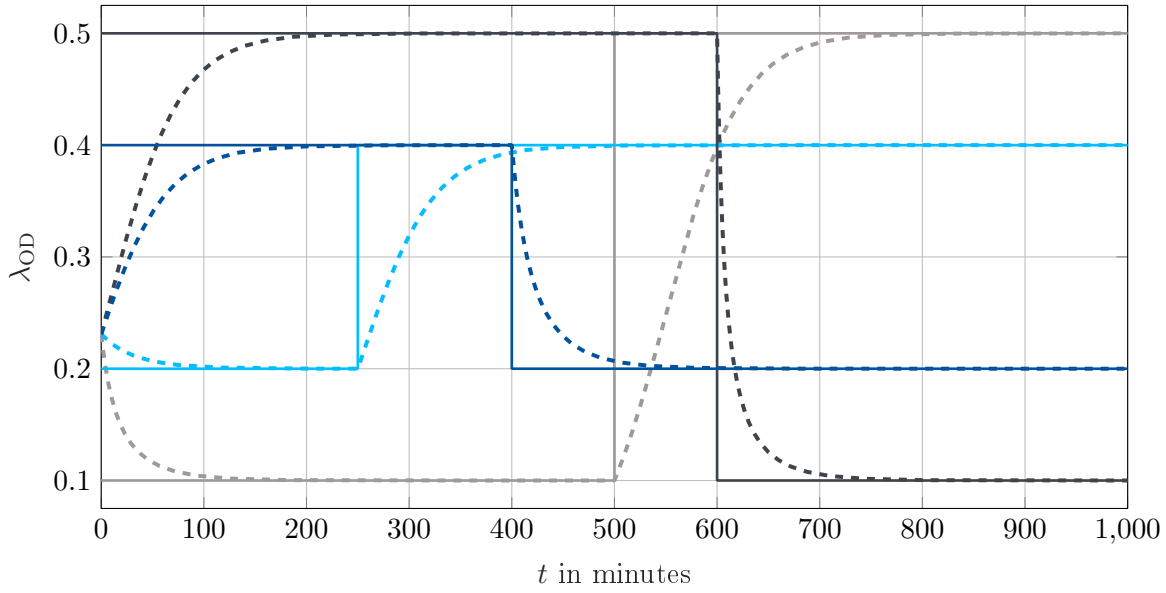

Figure 4.2: Reference and optimal trajectory of the OD with direct implementation of the controller output for reactor 1 (—/- - -), reactor 2 (—/- - -), reactor 3 (—/- - -) and reactor 4 (—/- - -).

4.3.3 Results

The mean error for all strategies and reactors is shown in Figure 4.3. It lies between $0.83 \cdot 10^{-3}$ and $5.18 \cdot 10^{-3}$. Thus, in all cases, the error is in the single-digit percentage range of the references for OD, which are between 0.1 and 0.5. For all reactors, the interval strategy in operation with one pump (IS 1P) has by far the highest error. It is about twice as high as the second highest error for all reactors. The highest demand strategy in operation with two pumps (HDS 2P) is the strategy with the smallest error for all reactors followed by the interval strategy for two pumps (IS 2P). For operation with one pump, the highest demand strategy with and without minimum quantity are about the same for all reactors. Compared to the best strategy for two pumps, the operation with the best strategy with one pump results in about twice the error. Figure 4.4 shows the simulation results for the strategy with the highest error (IS 1P) and with the lowest error (HDS 2P). It can be seen that the error is small compared to the reference variables, especially for the strategy with the smallest error. The effect of taking samples every 15 minutes can be seen in the deflections for the IS 1P strategy that occur in this interval.

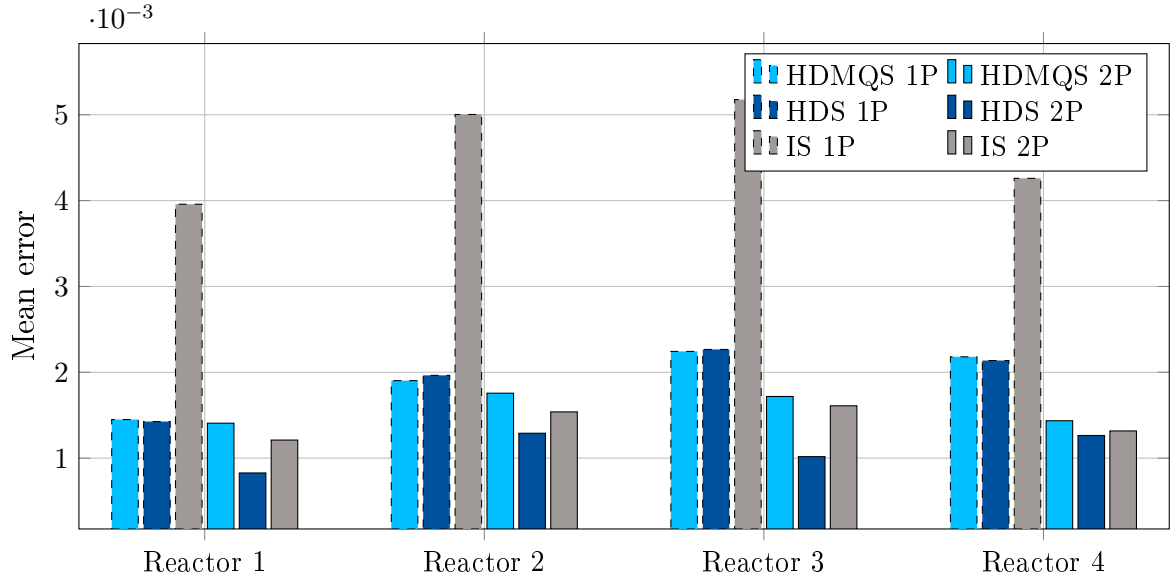

Figure 4.3: Mean error of the OD for every strategy and reactor.

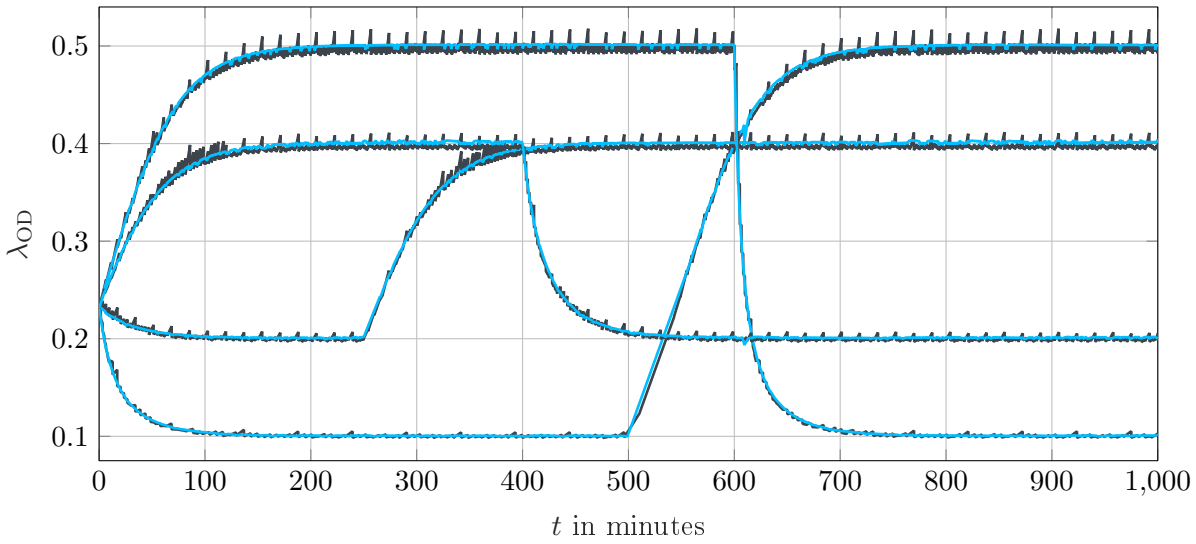

Figure 4.4: Simulation results of the OD experiment using the best performing HDS 2P strategy(—) and worst performing IS 1P(—) strategy.

Chapter 5

Prototype for four bioreactors

The goal of the prototype for four bioreactors is to perform the first biological experiments using a millifluidic system. In doing so, the control software and fluid management strategies can be improved and the simulator from chapter 4 can be validated. In addition, a concept for sterility can be tested. In section 5.1, the design is described followed by the functions possible with the board in section 5.2. The manufacturing and assembly process is explained in section 5.3.

As with the validation prototype from chapter 3, membrane valves are selected as the valve principle and laser machining as the manufacturing process.

5.1 Design

The design of flow layer and control layer is shown in figure 5.1. It is inspired by the millifluidic boards designed by Wong et al. [Won+18]. In area 1, up to four different inputs can be connected, e.g. substrates, cleaning liquids such as water or ethanol, or air to empty the channels. The inputs are opened and closed individually via four valves. If even more inputs are realized, multiplexing can be used to reduce the number of solenoid valves required. In area 2 there are output and input for the external peristaltic pump. In area 3 there is an output which is necessary for the operation with one pump. The return line in area 4 can be used for reactor-to-reactor transport or waste removal in operation with one pump. In area 5, one of the four lines to the four reactors is selected using demultiplexing of the volume flow. With four reactors, this does not yet save solenoid valves compared to a single control. Demultiplexing is nevertheless implemented to test the function. In area 6 are the connections for the supply lines to the reactors. The valves that close and open the feed lines are all controlled in parallel, as can be seen on the corresponding height in the control layer. In area 7 there is another set of valves to close the bypass line when the reactors are supplied. The bypass line is needed to be able to clean the inlet and outlet lines from the reactors. Area 8 contains the reactor outlet lines. Excess volume is removed and samples are taken through these. As with the inlet lines, all outlet lines can be opened or closed simultaneously. The reactor for a volume discharge is selected by multiplexing the valves in area 9. As with the feed lines, solenoid valves are not yet saved here

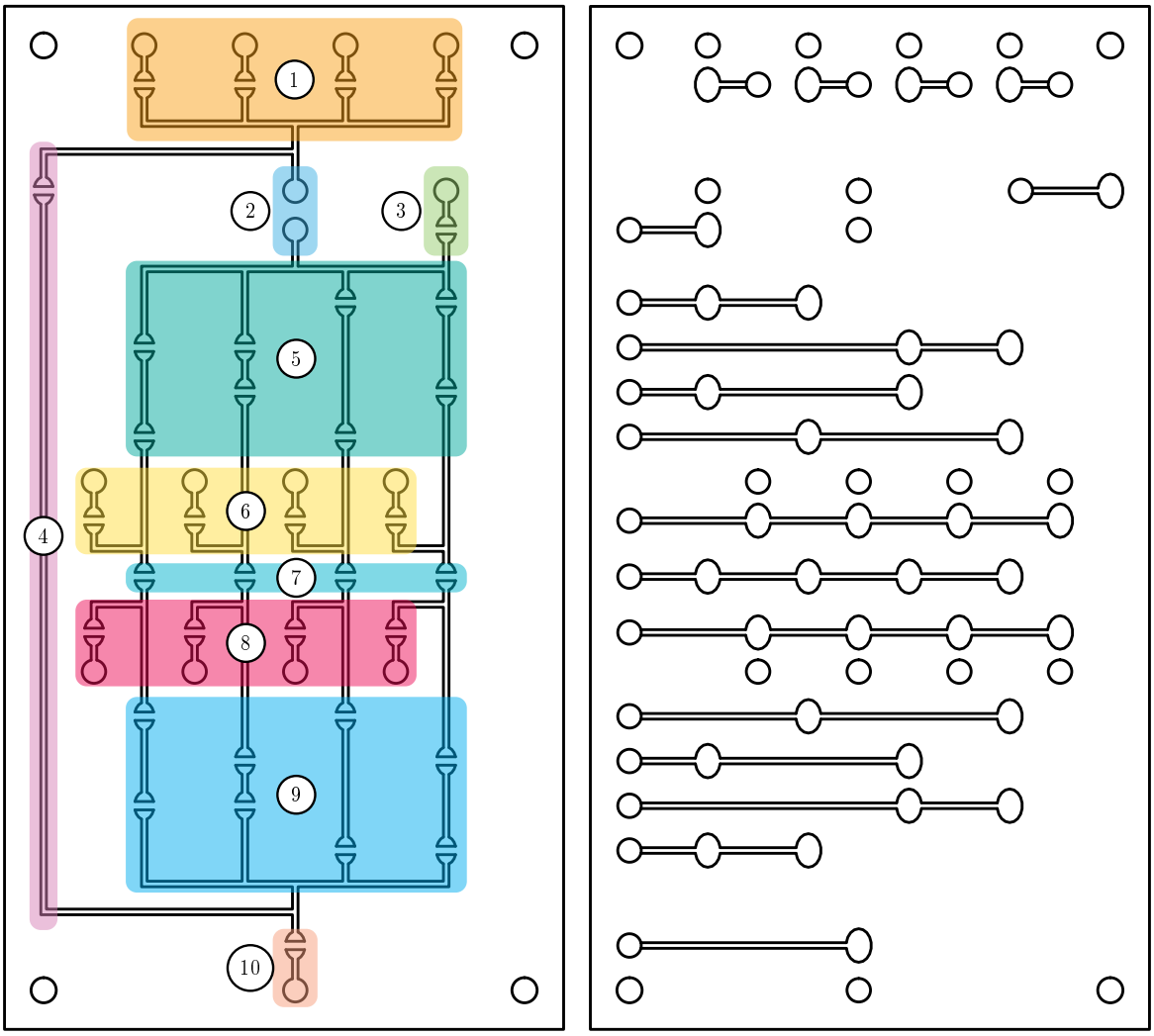

(a) Flow layer mit Markierung der verschiedenen Bereiche. **(b)** Control layer.

Figure 5.1: Design of the prototype for four bioreactors with marking of the different functional areas on the flow layer.

with four reactors, but multiplexing is still implemented for testing purposes. In area 10 is the output for the optional second pump for volume disposal and sampling. This output can be opened and closed with another valve.

5.2 Functionalities

A basic function of the millifluidic system is to supply the reactors with substrate. For this purpose, the input with the desired substrate is opened in area 1. The target reactor for the substrate is selected via suitable switching of the valves in area 5. The valves for the feed lines in area 6 are opened, the bypass lines in area 7 are closed. Activating the pump in area 2 starts the supply of substrate.

Another basic function of the millifluidic system is the waste removal of excess volume from the reactors. For this purpose, the bypass line is closed and the outlet lines in area 8 are opened.

Suitable switching of the valves in area 9 is used to select the reactor from which volume is to be removed. In operation with two pumps, the excess volume is extracted via the outlet in area 10 by the second pump. In operation with one pump, the valve of the return line in area 4 is opened and that of the additional outlet in area 3 is opened. All valves in area 5 are closed. In this way, the volume can be sucked out of the reactor via the pump in area 2 and removed from the system via the output in area 3.

Sample collection is performed in the same way as waste removal of excess volume. The separation between waste and samples after the exit is not part of this work and can be realized e.g. with another millifluidic board.

The cleaning of the supply and waste lines is done by selecting the input with the desired cleaning medium in area 1. In areas 5 and 9 the line to be cleaned is selected. The cleaning medium is pumped through the line via the pump in area 2. In operation with two pumps, the second pump in area 10 must run synchronously with the first and remove the cleaning medium. In operation with one pump, only the valve in area 10 must be opened and the outlet must also be connected to the waste container.

As a further function, the transport of a bacterial culture from one reactor to another can be realized, e.g. to prevent the formation of a biofilm if it remains too long in one reactor. For this purpose, the source reactor is selected by the valves in area 9. The target reactor is selected by the valves in area 5. The outlet in area 10 is closed and the return line in area 4 is opened. Then the transport can take place through the pump in area 2.

5.3 Manufacturing and assembly

The prototype for four bioreactors uses the same manufacturing process, material, and valve principle as the validation prototype from chapter 3. Due to the not completely even processing surface of the laser processing machine, different engraving depths occur during the production of flow and control layer, as the distance of the laser to the workpiece varies. For this reason, only the engraving is performed first and no cuts are made. Visual inspection is used to assess where the engraving depth is sufficient and where it is not. Additional engraving runs are then made in some areas as required. Due to the larger base area, the wrinkle-free application of the silicone membrane is significantly more difficult than with the validation prototype. Here, the small width of the 3M 91022 adhesive tape of 15 mm is used: The adhesive cover film is removed successively for one strip and the silicone membrane is then bonded to this strip. The assembly supports help with alignment at the beginning. Figure 5.2 shows the finished prototype. Unfortunately, it cannot be tested within the scope of this project because the necessary more complex pneumatic control system is not yet available.

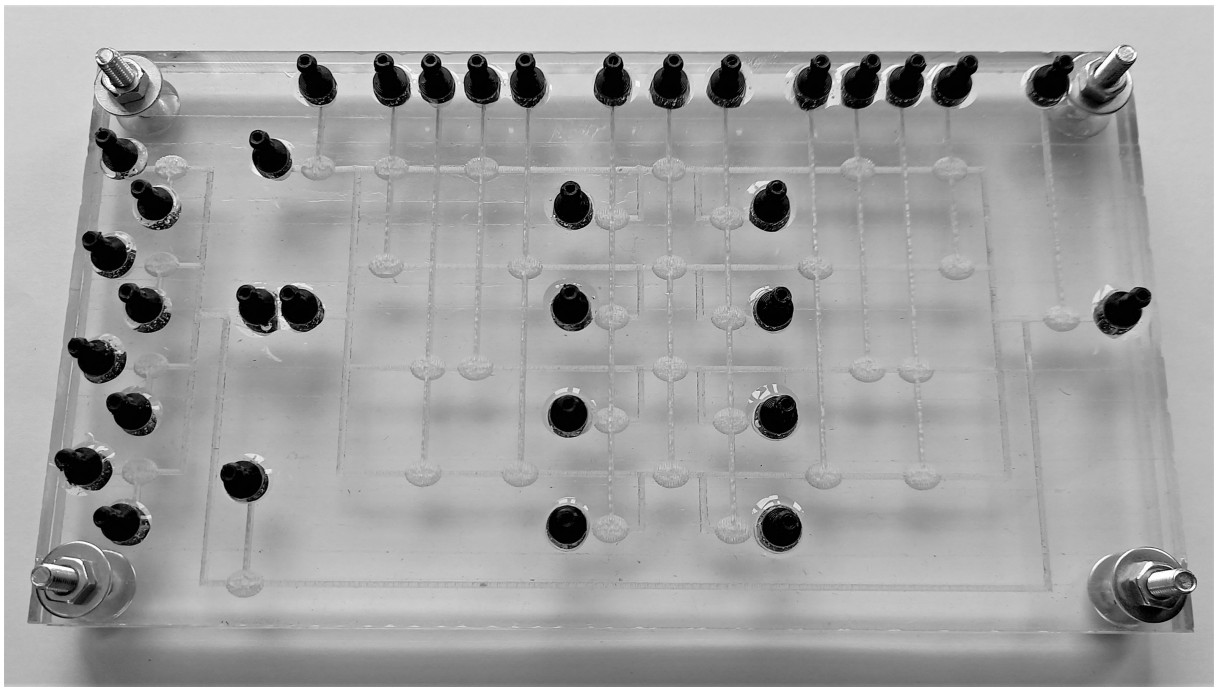

Figure 5.2: Assembled prototype for four bioreactors.

Chapter 6

Scalability

The prototype presented in chapter 5 is suitable for experiments with up to four bioreactors. Since experiments with more reactors will be performed in the future, this chapter shows how the millifluidic system can be scaled.

A non-modular approach to extending the prototype from chapter 5 would be to expand the number of outputs to the reactors on the board. As described in subsection 2.4.1, doubling the outputs to the reactors requires only two additional solenoid valves for pneumatic control. Exponential growth in the number of reactors causes only linear growth in the number of solenoid valves. The same applies to the number of inputs. With the expansion of the millifluidic board, the dimensions and complexity of manufacturing increase. If a mistake occurs during the laser machining process, a lot of material has to be disposed of. Also, the assembly, especially the accurate application of the silicone membrane to the flow layer, becomes much more challenging as the size increases.

For the above reasons, a modular approach to scaling the millifluidic system is preferred. In addition to simpler fabrication, this approach also offers significantly greater flexibility through the possible use of standardized, interchangeable submodules of the millifluidic system. Figure 6.1 shows a possible modular layout for a millifluidic system for up to 64 bioreactors and eight different inputs. Two pumps are foreseen for operation. The gray connections represent lines for fluids, and the light blue connections represent pneumatic connections. The dashed connection is an optional vial to vial line. In an 8 channel multiplexer, one of eight inputs is selected and connected to the output. In an 8 channel demultiplexer, one input is connected to one of eight outputs. However, the mechanical design is exactly the same for both, they are just used the other way around. When using the vial to vial function, the vial to vial line can be connected to one of the inputs of the 8 channel multiplexer board for input selection. The 8 channel multiplexer in the lower area must be extended by a second output for the use of a vial to vial function. Another unified board is the 8 channel reactor interface. It is constructed like areas 5 to 9 of the prototype for four reactors in figure 5.1 in chapter 5, except that instead of four channels eight channels are realized. The inlet and outlet tubes of up to eight reactors are connected to this board.

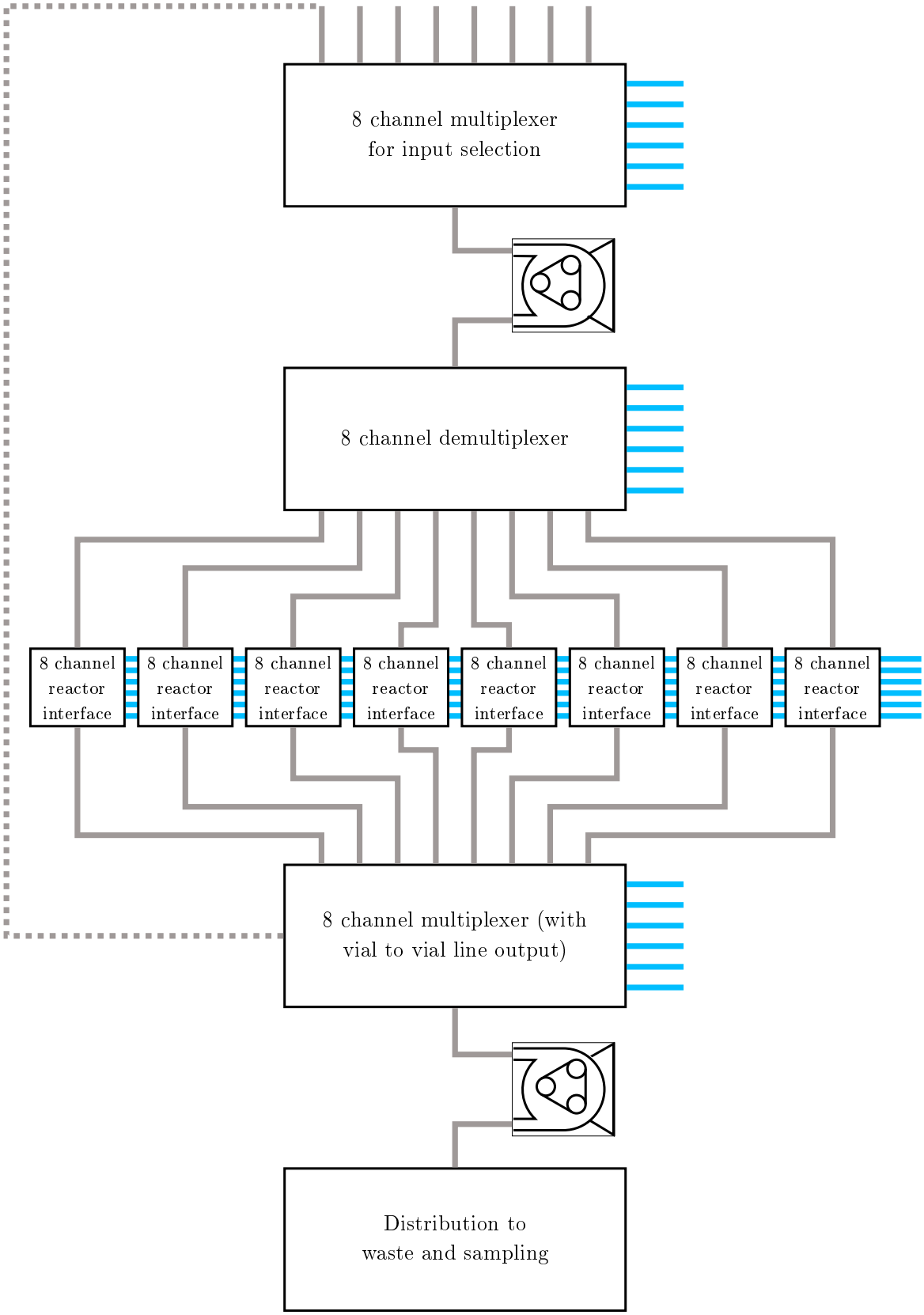

Figure 6.1: Example of a modular system for supplying up to 64 reactors with 8 inputs and vial to vial function. The system is operated with two pumps.

When the system is in operation, a substrate is selected from one of the eight inputs for supply. Via the pump, it enters the 8 channel demultiplexer, where it is distributed to one of up to eight 8 channel reactor interfaces. Within the interfaces, one of eight reactors is then selected for supply. All 8 channel reactor interfaces are controlled simultaneously. If e.g. reactor 1 is selected, reactor 1 will be selected on all of these boards. This is not a problem, because the corresponding board is already selected via the 8 channel demultiplexer. For waste removal and sampling, the same reactor is selected on all 8 channel reactor interface boards. The corresponding board is then selected via the 8 channel multiplexer in the lower area. The waste removal and sampling is done by the second pump. The separation of waste and samples can be done e.g. in another board. For the vial to vial function, the source reactor is selected for the outlet flow, the destination reactor for the inlet flow. At the 8 channel multiplexer for input selection, the vial to vial line is selected as the source. The transport is done by the upper pump.

If a vial to vial function is omitted and the same reactor can always be selected for supply and waste removal, demultiplexing and multiplexing can be synchronized to save valves for pneumatic control. The valves of the 8 channel demultiplexer are connected to the corresponding valves of the 8 channel multiplexer at the outlet. And the valves for internal multiplexing in the 8 channel reactor interfaces are connected to the corresponding valves of the internal demultiplexing.

Chapter 7

Conclusion and outlook

This work dealt with the design and fabrication of millifluidic boards for fluidic supply and volume removal of multiple bioreactors operated in parallel during biological experiments. A validation prototype was used to optimize the manufacturing process and design and to verify the basic functions. On this basis, a prototype for the operation of four bioreactors was designed and manufactured. In parallel, a simulator was developed to prepare and adjust the parameters of experiments with a millifluidic system and multiple bioreactors.

After the introduction and motivation of the thesis in chapter 1, the elaboration of the state of the art and the basics for the project was carried out in chapter 2. Millifluidics was distinguished from nano- and microfluidics. Various possible manufacturing processes for producing millifluidic systems and different valve designs for this scale were presented. Another section is devoted to hardware and software control of fluidic systems. Modeling and control of bioreactors as a basis for the simulator from chapter 4 conclude the chapter.

In chapter 3, the development, manufacturing, optimization and testing of the validation prototype were carried out. Laser machining was selected as the manufacturing process and membrane valves as the valve design method. The prototype was used to implement a simple Y-junction with two valves. This allowed the basic properties and functions of the millifluidic boards to be tested: The function of the valves, the tightness of the board at a flow rate, the choice between several inputs, draining of the channels and endurance resistance. In order to obtain a fully functional prototype, the design and manufacturing process had to be adjusted several times. Especially the adhesive bonding with the silicone with very low surface energy was a challenge. In the end, all tests could be carried out successfully. In addition to building and testing the prototype, the peristaltic pump used for the tests and for future experiments was calibrated.

In chapter 4, the simulator for biological experiments with a millifluidic system was developed. Six different fluid management strategies were formulated. Three are for operation with one pump, and three are for operation with two pumps. The simulator was applied to the prototype example from chapter 5. It was used to compare the fluid management strategies for an experiment with four bioreactors and to select the optimal strategy.

In chapter 5, the design and fabrication of a prototype for four bioreactors was done. Due to the size, the fabrication was more difficult compared to the validation prototype. Up to four different inputs are provided. Operation with one pump as well as with two pumps is possible. Other features include a vial-to-vial function and bypass lines between inputs and outputs to clean the system. Due to the unavailability of pneumatic control, this prototype could not be tested.

In chapter 6 aspects of the scalability of the approach were discussed. The layout of a system for up to 64 bioreactors and with up to 8 inputs was shown as an example. Modular, standardized components offer easier manufacturing and more flexibility in this context.

This work represented the beginning of the introduction and use of millifluidic systems for biological experiments at the Politechnic University of Valencia. Accordingly, many open fields regarding this topic exist that can be addressed in the future. Obviously, the prototype for four reactors from chapter 5 can be put into operation as soon as the pneumatic control system for it is available and set up. This will allow its operation to be verified. Biological experiments can then be performed with the prototype to gain initial experience in practical applications and to validate or, if necessary, adapt the simulator. For example, a multi-objective optimization for the different fluid management strategies could be set up to find the optimal parameters. The prototype can also be used to develop protocols to ensure and maintain sterility during experiments. For controlling the experiments, either the simulator control can be implemented on an Arduino or alternatively the software of Wong et al. [Won+18] can be adapted for one's own application. To improve the chemical properties of the millifluidic boards, the manufacturing process for the PETG material can be optimized to produce functional plates for future boards from this alternative material. To prevent leaks at the connections of the boards, suitable connectors (e.g. from Nordson Medical) can be obtained from the specialist laboratory trade, which could not be bought at the time of the project. Optimization of the design with respect to minimum distances between valves and lines can be carried out to save space and material costs.

Bibliography

[Ali09] M. Ali. "Fabrication of microfluidic channel using micro end milling and micro electrical discharge milling". In: *International Journal of Mechanical and Materials Engineering* 4 (2009) (cit. on p. 10).

[Ard+15] L. K. Ardila et al. "Micro-milling process for manufacturing of microfluidic moulds". In: 2015 (cit. on p. 10).

[BD91] G. Bastin and D. Dochain. "On-Line Estimation and Adaptive Control of Bioreactors". In: 1991 (cit. on pp. 14, 15).

[BIQ21] BIQU. *Red A4988 Stepper Motor Driver Board With Heatsinks*. `https://www.biqu.equipment/products/1pcs-3d-printer-kit-a4988-stepper-motor-driver-module-with-heatsinks-reprap-board-for-3d-printer-free-shipping`. [Online; accessed 15-January-2021]. 2021 (cit. on p. 23).

[BTM14] K. C. Bhargava, B. Thompson, and N. Malmstadt. "Discrete elements for 3D microfluidics". In: *Proceedings of the National Academy of Sciences* 111 (2014), pp. 15013–15018 (cit. on p. 9).

[Esm+19] Franziska M. Esmek et al. "Sculpturing wafer-scale nanofluidic devices for DNA single molecule analysis". In: *Nanoscale* 11 (28 2019), pp. 13620–13631. DOI: `10.1039/C9NR02979F` (cit. on p. 6).

[GKT16] Andreas Gebhardt, Julia Kessler, and Laura Thurn. *3D-Drucken: Grundlagen und Anwendungen des Additive Manufacturing (AM)*. Deutsch. 1 Online-Ressource (XVI, 218 Seiten). München, 2016 (cit. on pp. 7–9).

[GL13] N. Gao and X.J. Li. "5 - Controlled drug delivery using microfluidic devices". In: *Microfluidic Devices for Biomedical Applications*. Ed. by Xiujun (James) Li and Yu Zhou. Woodhead Publishing Series in Biomaterials. Woodhead Publishing, 2013, 167–185e (cit. on p. 5).

[Guc+15] D. J. Guckenberger et al. "Micromilling: a method for ultra-rapid prototyping of plastic microfluidic devices." In: *Lab on a chip* 15 11 (2015), pp. 2364–78 (cit. on p. 9).

[HQ03] C. Hansen and S. Quake. "Microfluidics in structural biology: smaller, faster ... better". In: *Current Opinion in Structural Biology* 13 (2003), pp. 538–544 (cit. on p. 7).

[ILH10] Tobias Illg, Patrick Löb, and Volker Hessel. "Flow chemistry using milli- and microstructured reactors - From conventional to novel process windows". In: *Bioorganic & Medicinal Chemistry* 18.11 (2010). Tetrahedron Young Investigator Award 2010: Professor Seeberger, pp. 3707–3719 (cit. on p. 5).

[Kar18] Vassili Karanassios. "Microfluidics and Nanofluidics: Science, Fabrication Technology (From Cleanrooms to 3D Printing) and Their Application to Chemical Analysis by Battery-Operated Microplasmas-On-Chips". In: *Microfluidics and Nanofluidics*. Ed. by Mohsen Sheikholeslami Kandelousi. Rijeka: IntechOpen, 2018. Chap. 1 (cit. on pp. 5, 6).

[Kim+08] Pilnam Kim et al. "Soft lithography for microfluidics: a review". In: *Biochip Journal* 2 (2008), pp. 1–11 (cit. on p. 7).

[Kin+14] Philip H. King et al. "Interdroplet bilayer arrays in millifluidic droplet traps from 3D-printed moulds." In: *Lab on a chip* 14 4 (2014), pp. 722–9 (cit. on p. 10).

[Kit+12] Philip J. Kitson et al. "Configurable 3D-Printed millifluidic and microfluidic 'lab on a chip' reactionware devices". In: *Lab Chip* 12 (18 2012), pp. 3267–3271 (cit. on pp. 5, 7).

[Lop+15] Raquel Lopes et al. "Low cost microfluidic device for partial cell separation: Micromilling approach". In: *2015 IEEE International Conference on Industrial Technology (ICIT)* (2015), pp. 3347–3350 (cit. on p. 10).

[Mas21] MaschinenReich. *XP88-ST01 Peristaltic Pump*. `http://www.maschinenreich.com/wp-content/uploads/2017/03/XP88-Manual-A4-170320.pdf`. [Online; accessed 15-January-2021]. 2021 (cit. on p. 23).

[Mor+16] Alex J. L. Morgan et al. "Simple and Versatile 3D Printed Microfluidics Using Fused Filament Fabrication". In: *PLOS ONE* 11.4 (Apr. 2016), pp. 1–17 (cit. on p. 8).

[OA06] K. Oh and C. Ahn. "A review of microvalves". In: *Journal of Micromechanics and Microengineering* 16 (2006) (cit. on p. 10).

[PY18] T. Pilizota and Y. Yang. “"Do It Yourself" Microbial Cultivation Techniques for Synthetic and Systems Biology: Cheap, Fun, and Flexible”. In: *Frontiers in Microbiology* 9 (2018) (cit. on p. 3).

[Sha+14] Aliaa I Shallan et al. “Cost-effective three-dimensional printing of visibly transparent microchips within minutes”. In: *Analytical chemistry* 86.6 (2014), pp. 3124–3130 (cit. on p. 9).

[The20] The Lee Company. *Miniature solenoid valves, 2-port face mount: conventional models, Cross Section View.* `https://www.theleeco.com/products/electro-fluidic-systems/solenoid-valves/control-valves/lhd-series/2-port/face-mount/`. [Online; accessed 21-December-2020]. 2020 (cit. on p. 10).

[TJA79] S. C. Terry, J. H. Jerman, and J. B. Angell. “A gas chromatographic air analyzer fabricated on a silicon wafer”. In: *IEEE Transactions on Electron Devices* 26.12 (1979), pp. 1880–1886 (cit. on p. 10).

[Tsu+15] Soichiro Tsuda et al. “Customizable 3D Printed ’Plug and Play’ Millifluidic Devices for Programmable Fluidics”. In: *PLOS ONE* 10.11 (Nov. 2015), pp. 1–13 (cit. on pp. 6, 7, 11).

[VOE95] C. Vicider, O. Ohman, and H. Elderstig. “A Pneumatically Actuated Micro Valve With A Silicone Rubber Membrane For Integration With Fluid-handling Systems”. In: *Proceedings of the International Solid-State Sensors and Actuators Conference - TRANSDUCERS ’95* 2 (1995), pp. 284–286 (cit. on p. 11).

[Whi+01] G. Whitesides et al. “Soft lithography in biology and biochemistry.” In: *Annual review of biomedical engineering* 3 (2001), pp. 335–73 (cit. on p. 7).

[Whi17] Joseph J. Whittenberg. “Micro- and millifluidic platforms for imaging agent synthesis”. In: 2017 (cit. on p. 6).

[Won+18] B. Wong et al. “Precise, automated control of conditions for high-throughput growth of yeast and bacteria with eVOLVER”. In: *Nature biotechnology* 36 (2018), pp. 614–623 (cit. on pp. 3, 6, 7, 9, 11–14, 45, 54).

[XW98] Y. Xia and G. Whitesides. “Soft Lithography.” In: *Angewandte Chemie* 37 5 (1998), pp. 550–575 (cit. on p. 7).

[Zhu+15] F. Zhu et al. “Three-dimensional printed millifluidic devices for zebrafish embryo tests.” In: *Biomicrofluidics* 9 4 (2015), p. 046502 (cit. on p. 9).

Part II

Budget

Chapter 8

Budget

In this chapter the costs of the project are calculated. In section 8.1 the costs for the different work steps and prototypes are calculated. In section 8.2 the costs for the workforce are calculated. The summation of the total costs is done in section 8.3.

8.1 Budget breakdown

In this section, the costs for individual components and work steps are calculated, but without the working time. The working time is calculated separately. The costs shown include sales tax in each case.

Table 8.1 shows the costs for determining the parameters for laser processing. This step was done in subsection 3.3.1.

Table 8.1: Cost of parameter tuning of the laser processing machine.

Amount	**Unit**	**Item**	**Cost p.u. (€)**	**Cost (€)**
300	cm^2	PETG material, 8 mm	0.02266	6.80
150	cm^2	PETG material, 8 mm	0.01443	2.16
150	cm^2	Silicone rubber sheet, 0.2 mm	0.00276	0.41
200	cm^2	3M 9088 adhesive tape	0.00122	0.24
30	min	Iberolaser IL-9060 processing time	0.4	12
			Total	**21.61**

Table 8.2 shows the cost of manufacturing the validation prototype of Archicercle from PETG in subsection 3.5.1.

Table 8.2: Cost of the first validation prototype made out of PETG by Archicercle.

Amount	Unit	Item	Cost p.u. (€)	Cost (€)
1	ea.	Manufacturing of control and flow layer including the adhesive	150	150
70	cm^2	Silicone rubber sheet, 0.2 mm	0.00276	0.19
4	ea.	M4x25 screw	0.075	0.3
4	ea.	M4 nut	0.0375	0.15
8	ea.	Plain washer for M4 screws	0.01873	0.15
5	ea.	3D printed barbed adapter	0.05	0.25
0.5	g	Loctite EA 3430 epoxy adhesive	0.61179	0.31
			Total	**151.35**

Table 8.3 shows the cost of manufacturing the first validation prototype from in-house production using PMMA with 3M 9088 adhesive. This work was performed in subsection 3.5.2.

Table 8.3: Cost of the first validation prototype made out of PMMA using the adhesive tape 3M 9088.

Amount	Unit	Item	Cost p.u. (€)	Cost (€)
70	cm^2	PMMA material, 6 mm	0.01443	1.01
70	cm^2	3M 9088 adhesive tape	0.00122	0.09
6	min	Iberolaser IL-9060 processing time	0.4	2.4
70	cm^2	Silicone rubber sheet, 0.2 mm	0.00276	0.19
4	ea.	M4x25 screw	0.075	0.3
4	ea.	M4 nut	0.0375	0.15
8	ea.	Plain washer for M4 screws	0.01873	0.15
5	ea.	3D printed barbed adapter	0.05	0.25
0.5	g	Loctite EA 3430 epoxy adhesive	0.61179	0.31
			Total	**4.85**

Table 8.4 shows the cost of manufacturing the second validation prototype from in-house production using PMMA with 3M 91022 adhesive. This work was performed in subsection 3.5.3.

Table 8.4: Cost of the second validation prototype made out of PMMA using the adhesive tape 3M 91022.

Amount	Unit	Item	Cost p.u. (€)	Cost (€)
70	cm^2	PMMA material, 6 mm	0.01443	1.01
70	cm^2	3M 91022 adhesive tape	0.00748	0.52
6	min	Iberolaser IL-9060 processing time	0.4	2.4
70	cm^2	Silicone rubber sheet, 0.2 mm	0.00276	0.19
4	ea.	M4x25 screw	0.075	0.3
4	ea.	M4 nut	0.0375	0.15
8	ea.	Plain washer for M4 screws	0.01873	0.15
5	ea.	3D printed barbed adapter	0.05	0.25
0.5	g	Loctite EA 3430 epoxy adhesive	0.61179	0.31
			Total	**5.28**

Table 8.5 shows the costs for the equipment for testing the validation prototypes. For the pneumatic control, existing equipment from the laboratory is used, which is why these costs are not included. The tests were performed in section 3.5.

Table 8.5: Cost of the equipment for the validation prototype tests.

Amount	Unit	Item	Cost p.u. (€)	Cost (€)
1	ea.	XP88-ST01 peristaltic pump	50	50
1	ea.	Arduino Mega 2560	39.94	39.94
1	ea.	A4988 stepper motor driver	0.46	0.46
1	ea.	12V 2A power supply	7.87	7.87
1	ea.	Few resistors and a capacitor	0.3	0.3
2	m	Electrical wiring	0.025	0.05
2	m	Silicone tubing	1.5	3
			Total	**101.62**

Table 8.6 shows the cost of manufacturing the prototype for four reactors made in-house from PMMA with 3M 91022 adhesive. This process is described in section 5.3.

Table 8.6: Cost of the prototype for four bioreactos made out of PMMA using the adhesive tape 3M 91022.

Amount	**Unit**	**Item**	**Cost p.u. (€)**	**Cost (€)**
430	cm^2	PMMA material, 6 mm	0.01443	6.20
430	cm^2	3M 91022 adhesive tape	0.00748	3.22
120	min	Iberolaser IL-9060 processing time	0.4	48
430	cm^2	Silicone rubber sheet, 0.2 mm	0.00276	1.19
4	ea.	M4x25 screw	0.075	0.3
4	ea.	M4 nut	0.0375	0.15
8	ea.	Plain washer for M4 screws	0.01873	0.15
34	ea.	3D printed barbed adapter	0.05	1.70
3	g	Loctite EA 3430 epoxy adhesive	0.61179	1.84
			Total	**78.05**

8.2 Workforce

The cost of the workforce includes the work time of the student performing the work as well as the supervisor. The costs are shown in table 8.7.

Table 8.7: Cost of the workforce.

Amount	Unit	Item	Cost p.u. (€)	Cost (€)
440	h	Mechatronic engineer (student, post-graduate)	30	13200
30	h	Electronical engineer (tutor, PhD candidate)	45	1350
			Total	**14550**

8.3 Total cost of the project

Table 8.8 shows the total cost of the project. For this, the costs from section 8.1 and section 8.2 are added.

Table 8.8: Total cost of the project.

Amount	Unit	Item	Cost p.u. (€)	Cost (€)
1	ea.	Parameter tuning of the laser processing machine	21.61	21.61
1	ea.	Validation prototype made from PETG by Archicercle	151.35	151.35
1	ea.	Validation prototype made from PMMA in-house using 3M 9088 adhesive	4.85	4.85
1	ea.	Validation prototype made from PMMA in-house using 3M 91022 adhesive	5.28	5.28
1	ea.	Equipment for the validation prototype tests	101.62	101.62
1	ea.	Prototype for four bioreactos made from PMMA in-house using 3M 91022 adhesive	78.05	78.05
1	ea.	Workforce of the student and the supervisor	14550	14550
			Total	**14912.76**

Part III

Drawings

Chapter 9

Drawings

In this chapter the technical drawings of the self-designed components of this thesis are shown. Page 70 shows the flow layer, page 71 the control layer of the final design of the validation prototype from chapter 3. Pages 72 and 73 show the flow and control layers of the prototype for four reactors from chapter 5. Page 74 contains the drawing of the 3D-printed adapter for connecting the millifluidic boards to the tubes. Page 75 contains the drawing of the adapter for reducing the tube diameter from the pneumatic system to the tubes of the millifluidic board. The 3D models and drawings can also be found in the GitHub repository under `https://github.com/sb2cl/MilifluidicBoard`.

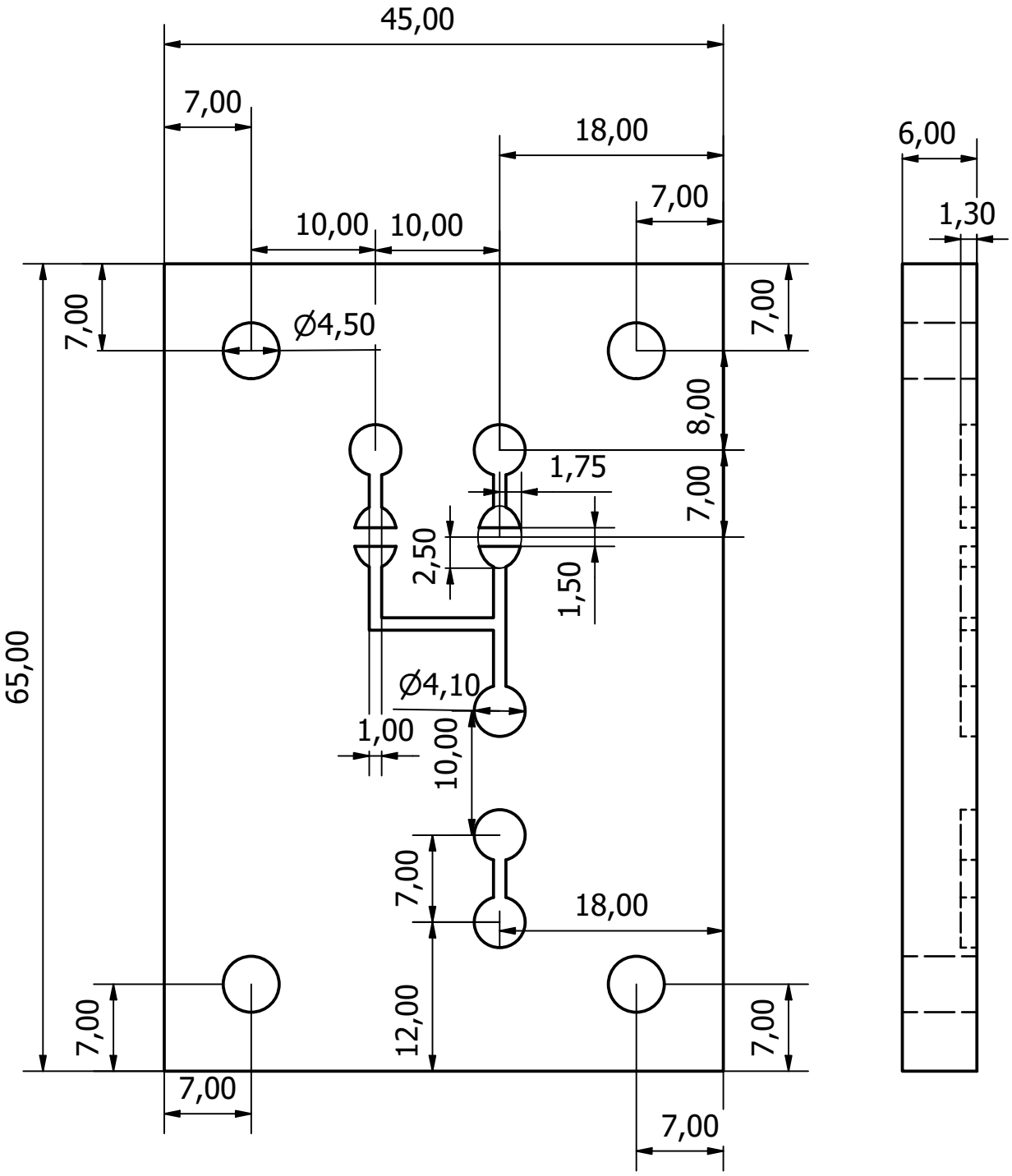

Designed by	Checked by	Approved by	Date		Date	
Nathan Beyer					19.08.2020	

	Validation prototype flow layer scale 2:1		
	Flow layer	Edition	Sheet 3 / 3

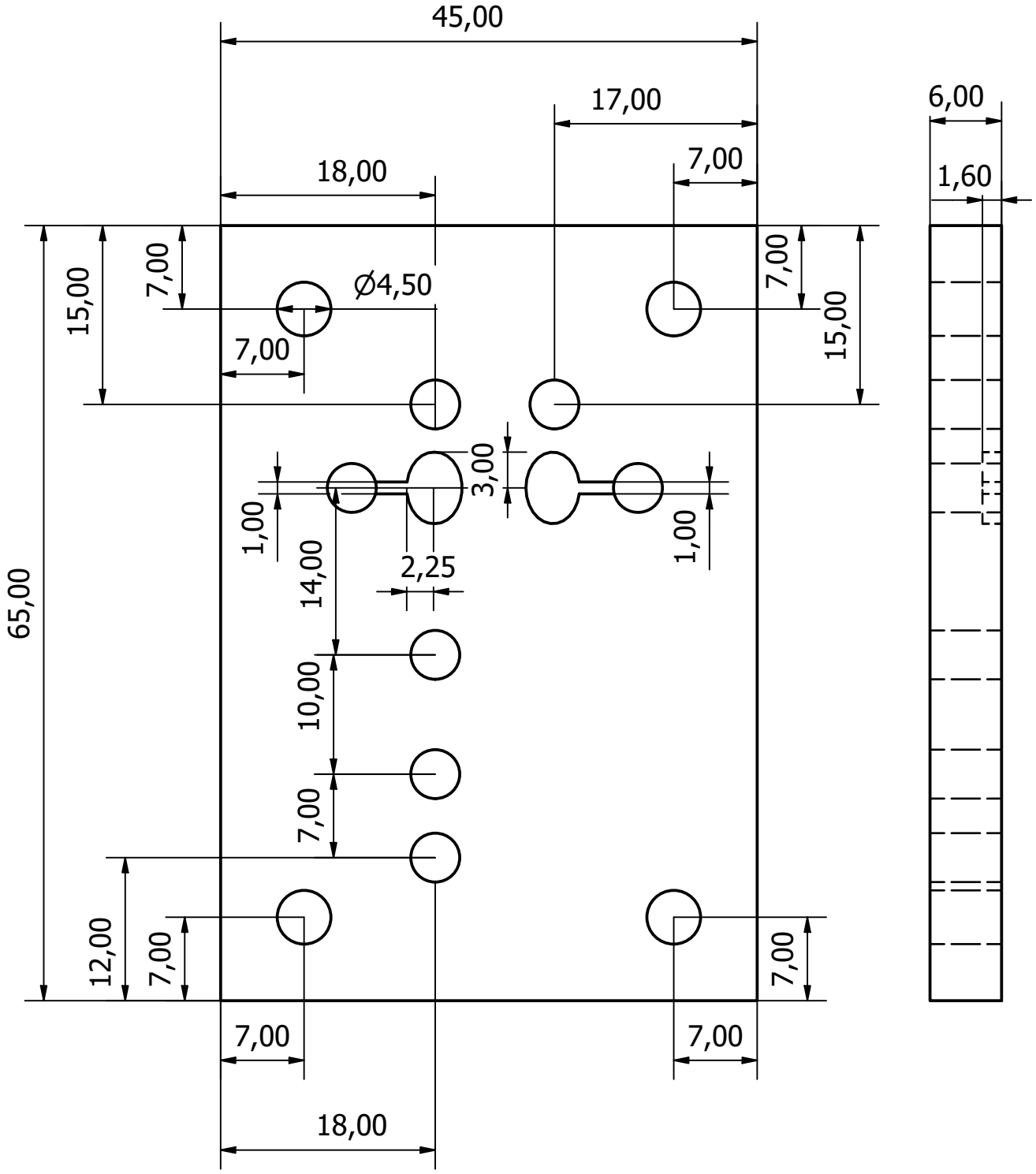

Designed by	Checked by	Approved by	Date		Date	
Nathan Beyer					19.08.2020	

	Validation prototype control layer scale 2:1		
	Control layer	Edition	Sheet 3 / 3

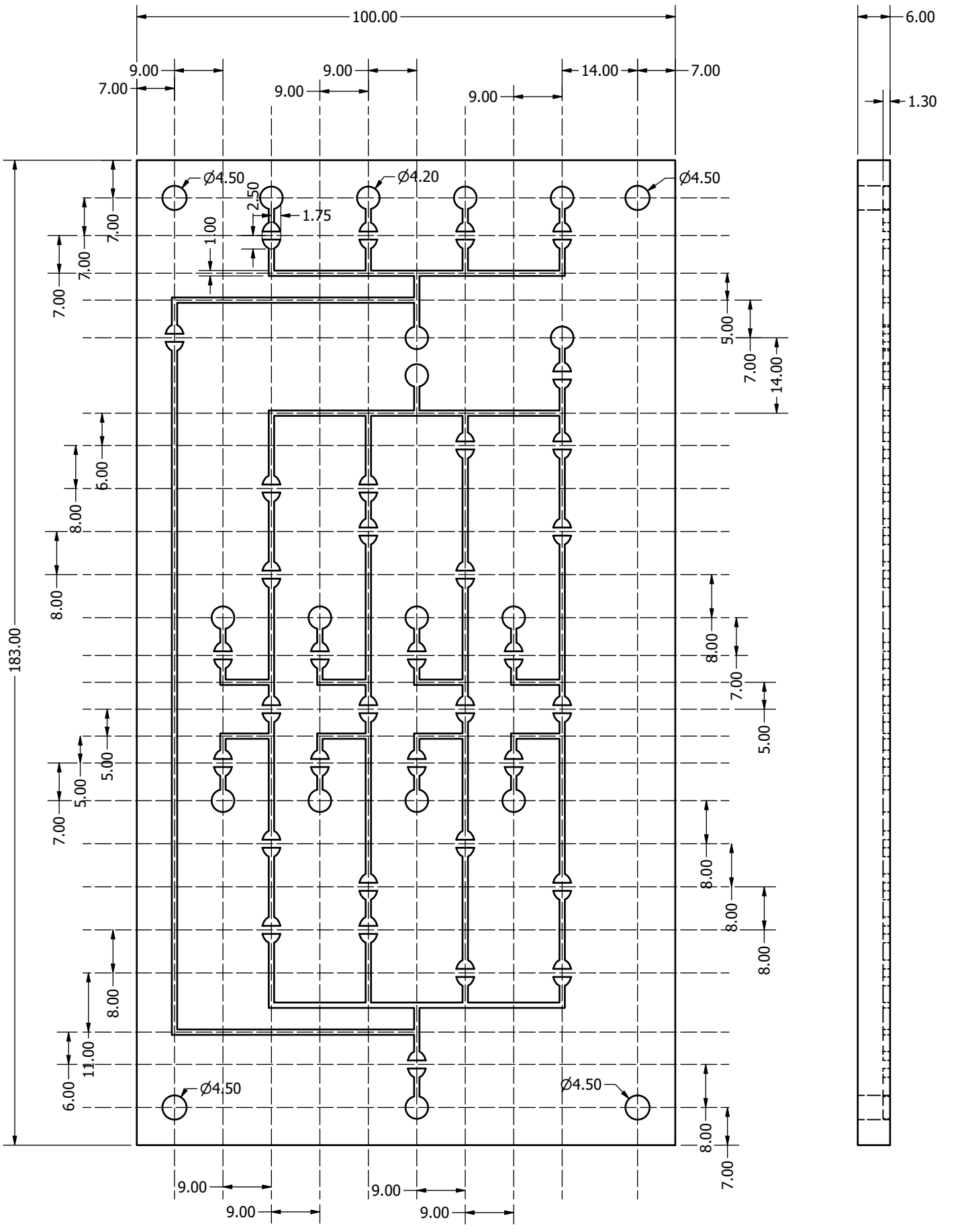

Designed by	Checked by	Approved by	Date	Date	
Nathan Beyer				31.07.2020	

	Prototype four reactors flow layer scale 3:2		
	Flow Layer	Edition	Sheet 3 / 4

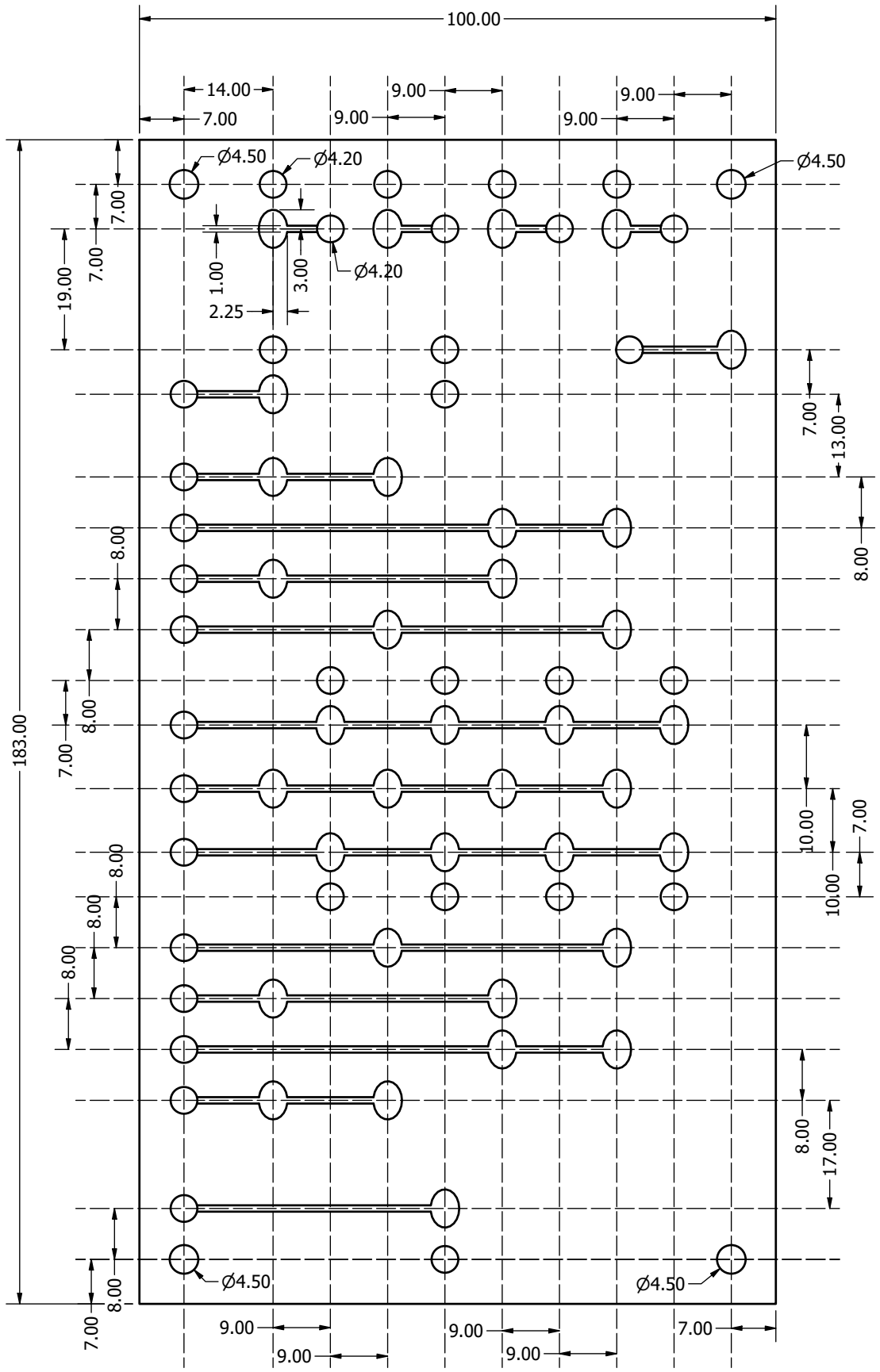

Designed by	Checked by	Approved by	Date		Date	
Nathan Beyer					31.07.2020	

Prototype four reactors control layer scale 3:2

Control Layer

Edition

Sheet 3 / 4

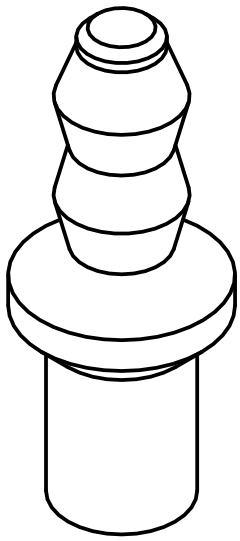

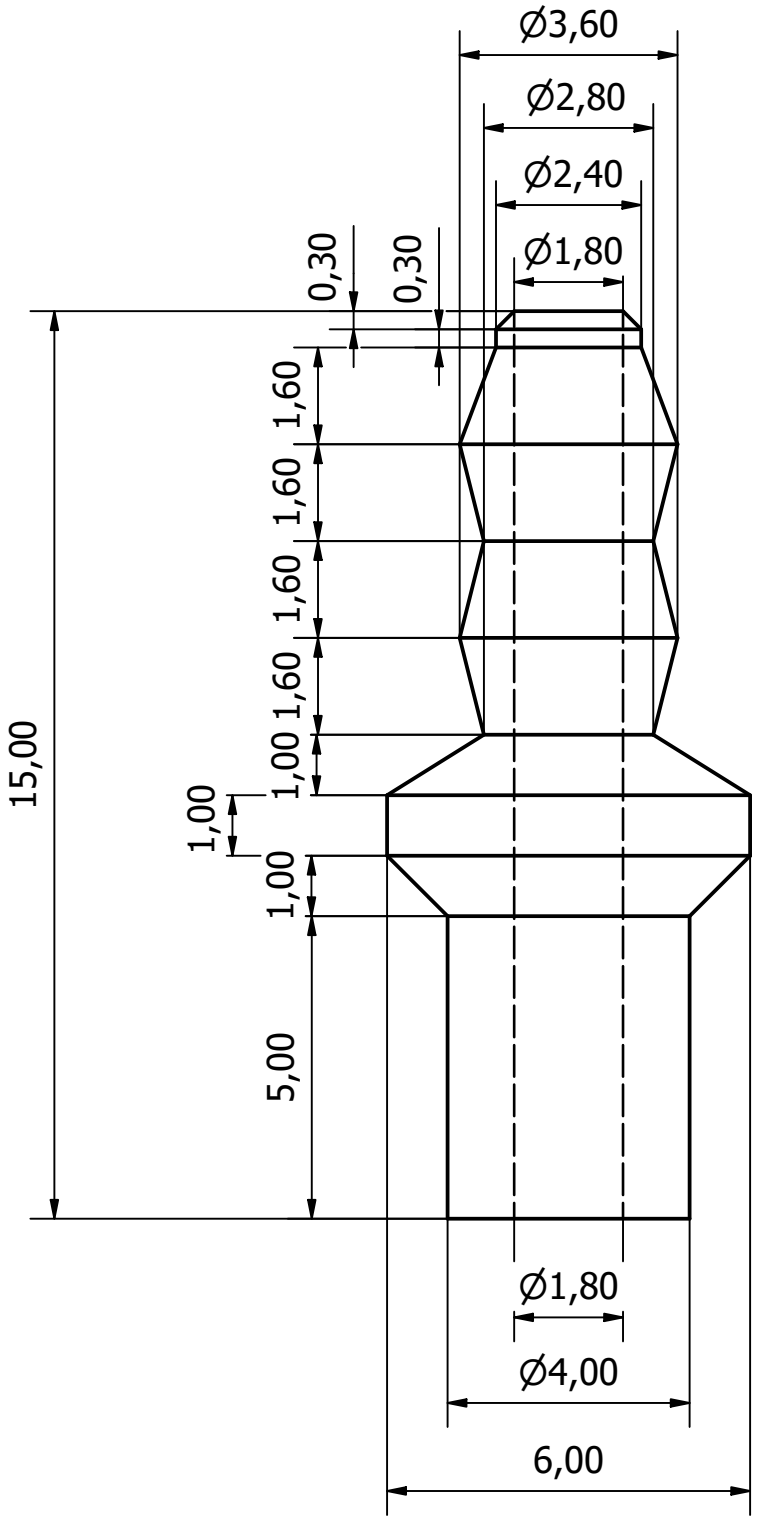

Designed by	Checked by	Approved by	Date		Date	
Nathan Beyer					11.01.2021	

	Hole to 2.4mm tube connector scale 8:1		
	Hole to barbed connector	Edition	Sheet 1 / 1

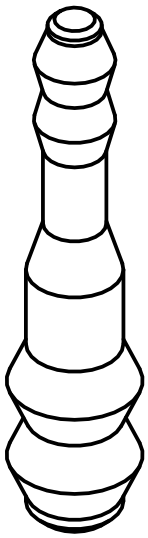

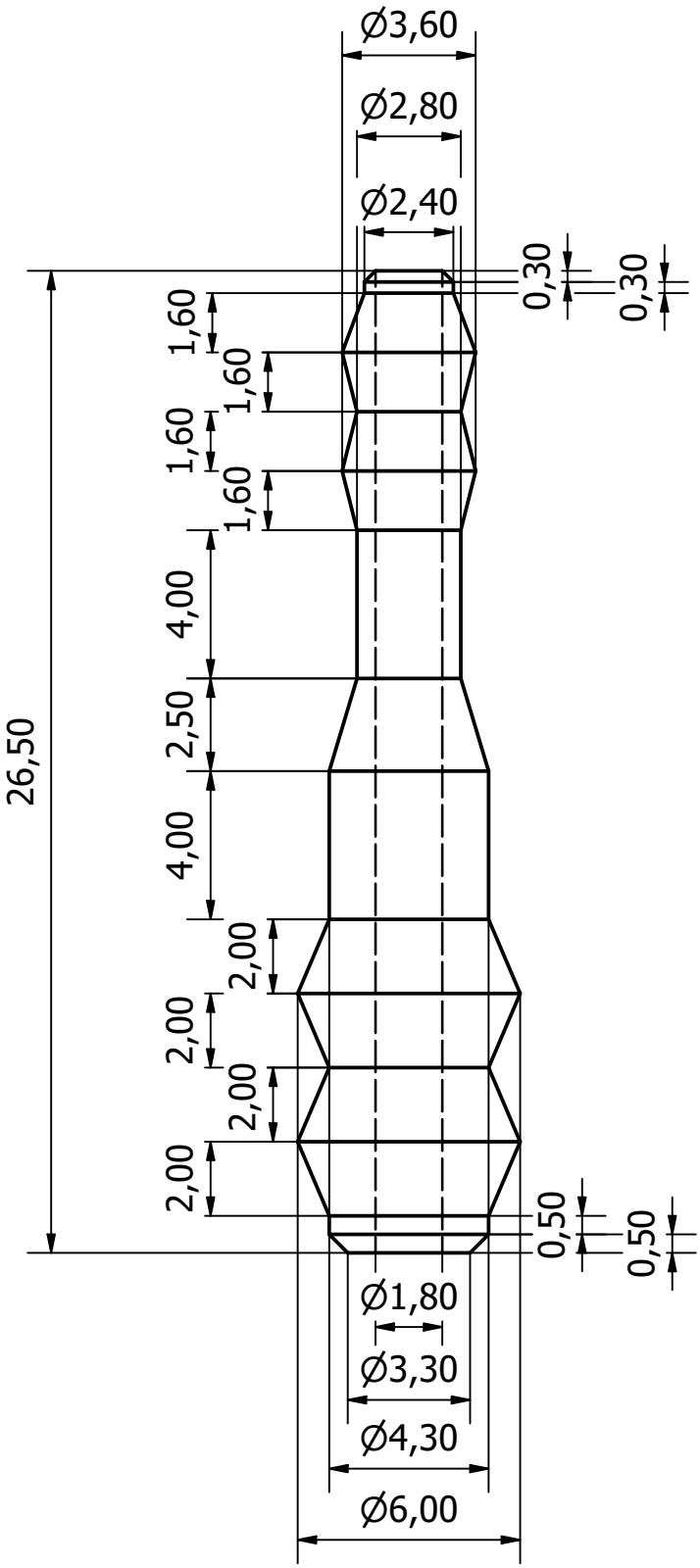

Designed by	Checked by	Approved by	Date		Date	
Nathan Beyer					11.01.2021	

	Tube to tube connector scale 5:1		
	Tube to tube connector	Edition	Sheet 1 / 1